

Mixture-Weighted Ensemble Kalman Filter with Quasi-Monte Carlo Transport

Ilja Klebanov¹ Claudia Schillings¹ Dana Wrischnig¹

January 28, 2026

Abstract. The Bootstrap Particle Filter (BPF) and the Ensemble Kalman Filter (EnKF) are two widely used methods for sequential Bayesian filtering: the BPF is asymptotically exact but can suffer from weight degeneracy, while the EnKF scales well in high dimension yet is exact only in the linear–Gaussian case. We combine these approaches by retaining the EnKF transport step and adding a principled importance-sampling correction.

Our first contribution is a general importance-sampling theory for *mixture* targets and proposals, including variance comparisons between individual- and mixture-based estimators. We then interpret the stochastic EnKF analysis as sampling from explicit Gaussian-mixture proposals obtained by conditioning on the current or previous ensemble, which leads to six self-normalized IS-EnKF schemes. We embed these updates into a broader class of ensemble-based filters and prove consistency and error bounds, including weight-variance comparisons and sufficient conditions ensuring finite-variance importance weights.

As a second contribution, we construct transported quasi-Monte Carlo (TQMC) point sets for the Gaussian-mixture laws arising in prediction and analysis, yielding TQMC-enhanced variants that can substantially reduce sampling error without changing the filtering pipeline.

Numerical experiments on benchmark models compare the proposed mixture-weighted and TQMC-enhanced filters, showing improved filtering accuracy relative to BPF, EnKF, and the standard weighted EnKF, and that the weighted schemes eliminate the EnKF error plateau often caused by analysis–target mismatch.

Keywords. Data assimilation • Sequential Bayesian filtering • Ensemble Kalman filter • Importance sampling • Gaussian mixture • Transported quasi-Monte Carlo

2020 Mathematics Subject Classification. 60G35 • 62M05 • 65C35 • 65C05 • 62F15

1. Introduction

Sequential Bayesian filtering aims to approximate the filtering distribution $p(x_t|Y_t)$ for a latent state sequence $(x_t)_{t \in \mathbb{N}_0}$ in \mathbb{R}^d generated by a stochastic state-evolution model, given observations $Y_t = (y_1, \dots, y_t)$. Particle methods approximate this distribution by a finite *ensemble* represented as a (possibly weighted) empirical measure,

$$p(x_t|Y_t) \approx \sum_{i=1}^N w_t^{(i)} \delta_{x_t^{(i)}}, \quad \sum_{i=1}^N w_t^{(i)} = 1,$$

where δ_x denotes the Dirac measure at x .

¹Freie Universität Berlin, Arnimallee 6, 14195 Berlin, Germany
 (ilja.klebanov@fu-berlin.de, c.schillings@fu-berlin.de, dana.wrischnig@fu-berlin.de)

Table 1.1: Comparison of the Bootstrap Particle Filter (BPF) and the Ensemble Kalman Filter (EnKF).

	BPF	EnKF
PREDICTION	Propagate the ensemble $(x_{t-1}^{(i)})_{i=1}^N$ through the dynamics with process noise to obtain the forecast (prior) ensemble $(\hat{x}_t^{(i)})_{i=1}^N$.	
Transport	$\tilde{x}_t^{(i)} = \hat{x}_t^{(i)}$ (no transport)	Prior particles $(\hat{x}_t^{(i)})_{i=1}^N$ are shifted to the posterior states $\tilde{x}_t^{(i)}$.
ANALYSIS		
Reweight & Resample	Weight by likelihood, normalize, then resample to obtain equally weighted $x_t^{(i)}$.	$x_t^{(i)} = \tilde{x}_t^{(i)}$ (no reweighting or resampling)

Most sequential filters operate by iterating a two-stage cycle—*prediction* followed by *analysis* (or *update*). The prediction step is essentially the same across methods: propagate the ensemble $(x_{t-1}^{(i)})_{i=1}^N$ through the dynamics with process noise to obtain the forecast (prior) ensemble $(\hat{x}_t^{(i)})_{i=1}^N$. The methods then differ primarily in the analysis step, where the new observation y_t is incorporated via a Bayesian update. Two canonical realizations of this paradigm are the Bootstrap Particle Filter (BPF; [Chopin and Papaspiliopoulos 2020](#); [Doucet et al. 2001](#); [Gordon et al. 1993](#)) and the Ensemble Kalman Filter (EnKF; [Evensen 1994, 2003](#)); [Table 1.1](#) contrasts their update cycles (see [Section 5](#) for details). In the analysis step, the BPF performs no transport ($\tilde{x}_t^{(i)} = \hat{x}_t^{(i)}$) but corrects toward the data via likelihood-based reweighting followed by resampling. This yields consistency under broad conditions, yet can suffer from weight degeneracy and large Monte Carlo variance, especially in high dimensions. The EnKF, by contrast, *transports* the forecast particles to analysis (posterior) states $(\tilde{x}_t^{(i)})$ using a Kalman-type gain K_t , typically retains equal weights, and omits resampling, an approach that scales well but is exact only in the linear-Gaussian setting and may be biased otherwise. Both particle filters and ensemble Kalman filters face challenges in high-dimensional problems; in the EnKF, practical applicability can often be achieved through covariance localization, cf. [Morzfeld et al. \(2017\)](#).

In this work, we leverage the complementary strengths of both paradigms: we retain the EnKF’s transport to steer particles toward regions of high posterior density, and we restore a principled correction via importance sampling (IS), optionally followed by resampling, thereby combining the EnKF’s computational efficiency with the posterior accuracy of particle methods while mitigating weight degeneracy as well as biases due to nonlinearities and non-Gaussianity, as illustrated by the following diagram:

In order to perform an importance-reweighting step, one must specify the proposal distribution explicitly—i.e., the law from which the transported particles $(\tilde{x}_t^{(i)})$ are actually sampled. A well-established choice is the *weighted EnKF* (WEKF; [Papadakis et al. 2010](#); [van Leeuwen et al. 2019](#)), which treats each particle separately and takes as proposal the conditional law on the *previous* ensemble,

$$q_{p,t}^{(i)} = p(\tilde{x}_t^{(i)} | (x_{t-1}^{(j)})_{j=1}^N),$$

which admits a closed-form Gaussian expression when the observation function h is linear and the gain is constructed accordingly.

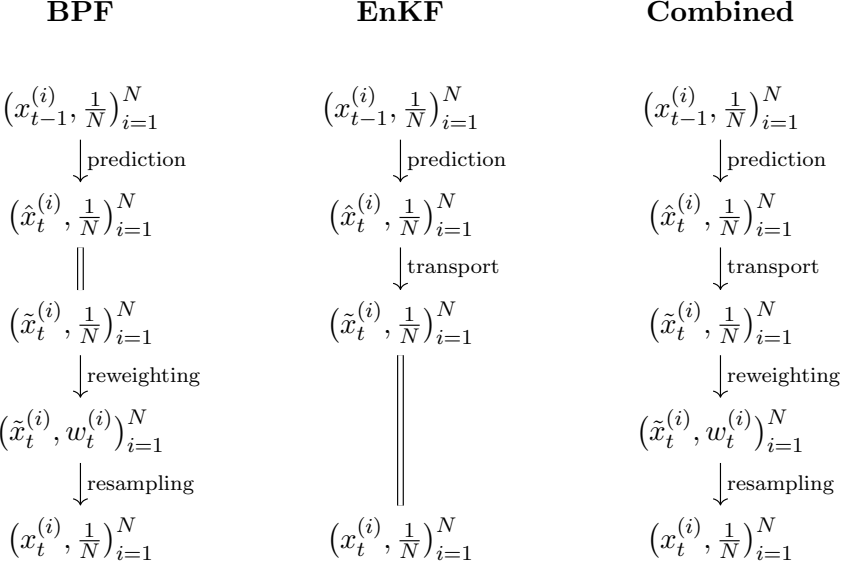


Figure 1.1: Schematic update at time t for the bootstrap particle filter (BPF), the ensemble Kalman filter (EnKF), and the combined scheme discussed in this paper. Conceptually, the combined scheme performs prediction, then transport, then reweighting and resampling. The BPF corresponds to skipping the transport step, while the EnKF corresponds to skipping the reweighting-and-resampling step.

In this paper we build on that paradigm and extend it in two complementary directions. First, beyond conditioning on the previous ensemble, we also work with the *current-ensemble* conditional

$$q_{c,t}^{(i)} = p(\tilde{x}_t^{(i)} \mid (\hat{x}_t^{(j)})_{j=1}^N),$$

which is available in closed form even for nonlinear h (Frei and Künsch, 2013b) and thereby supports importance reweighting for arbitrary observation functions. Second, we move from per-particle conditionals to *mixture formulations*: the transported ensemble can be viewed as a stratified (balanced) sample from the Gaussian mixtures

$$q_{p,t}^{\text{mix}} = \frac{1}{N} \sum_{i=1}^N q_{p,t}^{(i)} \quad \text{or} \quad q_{c,t}^{\text{mix}} = \frac{1}{N} \sum_{i=1}^N q_{c,t}^{(i)},$$

and similarly the Gaussian mixture prior induces a mixture target. Using these mixtures—rather than only the individual Gaussian components—leads to several novel *mixture-weighted* EnKF schemes that smooth across proposals and can thereby reduce weight variance.

Altogether, these choices (individual vs. mixture targets and proposals; conditioning on current vs. previous ensembles) yield six self-normalized IS (SNIS) schemes for the EnKF (one of them being WEnKF) that we analyze and compare, both theoretically and numerically.

A second main contribution of this paper is to replace the *random* generation of forecast and analysis ensembles by *transported quasi-Monte Carlo* (TQMC) point sets tailored to the Gaussian-mixture laws that arise in EnKF-type methods. Specifically, both the forecast ensemble $(\hat{x}_t^{(i)})_{i=1}^N$ and the transported ensemble $(\tilde{x}_t^{(i)})_{i=1}^N$ can be viewed as (stratified) samples from explicit Gaussian mixtures. Building on the transport framework of Klebanov and Sullivan (2023)—which provides an essentially closed-form map sending a reference density ρ_{ref} to any mixture of its affine transforms—we generate these ensembles by pushing low-discrepancy

point sets, e.g. randomized quasi-Monte Carlo (RQMC) points, through the corresponding mixture transports. This substitution preserves the algorithmic structure of BPF/EnKF (the prediction-analysis pipeline and the same target/proposal laws) while reducing sampling error: low-discrepancy point sets cover the state space more uniformly than independent random draws and, for sufficiently regular integrands, yield provably higher convergence rates than standard Monte Carlo (MC) or Markov chain Monte Carlo (MCMC) methodologies; see, e.g., [Owen \(2013\)](#). In our setting this manifests as lower variance of the corresponding empirical estimators and, consequently, more stable and accurate filtering, as confirmed by our numerical experiments.

Contributions. We make the following contributions.

- (C1) **Importance sampling with mixture targets and proposals.** In [Section 4](#) we develop a unified IS framework for *mixture* targets and *mixture* proposals. It yields several unbiased estimators (including stratified/balanced variants) together with variance comparisons that identify when mixture-based reweighting improves over per-component schemes. This theory motivates mixture-weighted reweighting in EnKF-type filters.
- (C2) **Explicit EnKF proposals via current- and previous-ensemble conditionals.** We cast the stochastic EnKF analysis step as sampling from explicit Gaussian proposals. For linear observations we introduce a *previous-ensemble* gain K_t^p , independent of the forecast noises, so that the *previous-ensemble* conditional $p(\tilde{x}_t^{(i)} \mid (x_{t-1}^{(j)})_{j=1}^N)$ is *exactly* Gaussian, addressing the mean-field caveat in the common WEnKF construction. For general (possibly nonlinear) h we formalize the *current-ensemble* conditional $p(\tilde{x}_t^{(i)} \mid (\hat{x}_t^{(j)})_{j=1}^N)$, which enables principled importance reweighting beyond the linear setting of the WEnKF.
- (C3) **Mixture-weighted EnKF schemes and consistency.** Combining (i) individual vs. mixture targets, (ii) individual vs. mixture proposals, and (iii) conditioning on current vs. previous ensembles yields six self-normalized IS-EnKF variants (including WEnKF as a special case). We prove consistency for all six schemes under a standard finite-variance condition on the IS weights ([Theorem 6.1](#)).
- (C4) **Weight-variance optimality and finite-variance conditions.** Let σ_t^2 denote the squared coefficient of variation of the (unnormalized) importance weights at time t (equivalently, the variance of the weights after rescaling them to have mean one), which controls the SNIS error bounds in our convergence proof. We show that σ_t is minimized (among our schemes) by using mixture targets together with mixture proposals ([Theorem 6.2](#)). Moreover, for linear h and under bounded drift f , we establish the key condition $\sigma_t < \infty$ required for consistency for two of the schemes considered ([Theorem 6.3](#)).
- (C5) **TQMC for Gaussian mixtures.** We propose replacing random sampling in both prediction and analysis by *transported quasi-Monte Carlo* (TQMC) for Gaussian mixtures ([Section 7](#)). This preserves the BPF/EnKF pipeline while lowering sampling error and stabilizing moment and gain estimates. We obtain TQMC-enhanced variants of BPF, EnKF, and their mixture-weighted variants, with substantial accuracy gains in low-to-moderate dimensions for consistent methods, while performing at least comparably in higher-dimensional tests.
- (C6) **Numerical evidence.** Across benchmarks, we find that mixture-based reweighting reduces weight degeneracy and improves estimation accuracy relative to per-component reweighting (including WEnKF-style baselines). Moreover, in regimes where the plain EnKF exhibits an N -independent error plateau due to analysis-target mismatch, the weighted schemes exhibit the expected decay with N .

Outline. After discussing related work and introducing notation in [Sections 2](#) and [3](#), [Section 4](#) develops a general importance-sampling theory for *mixture* targets and proposals, including variance comparisons between individual- and mixture-based estimators ([Theorem 4.1](#)). [Section 5](#) formulates the filtering setting and reviews the BPF/EnKF prediction–analysis pipeline, interpreting the stochastic EnKF analysis step as sampling from explicit Gaussian proposals obtained by ensemble conditioning and an appropriate gain construction. Building on this, [Section 6](#) introduces six self-normalized IS–EnKF schemes, summarized in [Table 6.1](#) and [Algorithm 2](#). [Section 6.1](#) embeds these methods into a broader class of ensemble-based filters—including localized and inflated variants—via a generic proposal mechanism, and [Section 6.2](#) establishes consistency and error bounds, including weight-variance comparisons ([Theorem 6.2](#)) and finite-variance conditions ([Theorem 6.3](#)). Next, [Section 7](#) presents transported quasi-Monte Carlo (TQMC) constructions for the Gaussian-mixture laws governing prediction and analysis, yielding TQMC-enhanced variants summarized in [Algorithm 4](#). Finally, [Section 8](#) compares the proposed mixture-weighted and TQMC-enhanced filters in numerical experiments on benchmark models, and [Section 9](#) concludes.

2. Related Work

The Ensemble Kalman Filter (EnKF) ([Evensen, 1994, 2003](#)) is widely used for sequential Bayesian estimation in high-dimensional systems. While computationally efficient, its Gaussian-linear assumptions lead to biased estimates in nonlinear or non-Gaussian settings. This has motivated a range of approaches that combine EnKF with particle filtering ideas.

Hybrid methods introduce importance weighting into the EnKF ([Frei and Künsch, 2013b; Hoteit et al., 2012](#)), but may suffer from weight degeneracy unless resampling is used. Transform-based approaches employ optimal transport ([Reich, 2013](#)), reducing degeneracy at higher computational cost. Gaussian mixture formulations ([Frei and Künsch, 2013a; Stordal et al., 2011](#)) aim to capture non-Gaussian features but scale less favorably in high dimensions.

Localization strategies have been proposed to improve scalability ([Chen et al., 2020; Robert and Künsch, 2017](#)), while further hybrid variants target specific regimes such as moderately non-Gaussian priors ([Grooms and Robinson, 2021](#)) or Lagrangian data assimilation ([Slivinski et al., 2015](#)). On the theoretical side, convergence and stability results have been established for ensemble Kalman particle filters ([Del Moral and Horton, 2023](#)) and optimal transport formulations of the EnKF ([Taghvaei and Mehta, 2021](#)). Comparative studies such as ([Pasetto et al., 2012](#)) further highlight trade-offs between EnKF and particle filter methods.

The present work builds on these developments by introducing mixture-based importance weighting strategies for the EnKF. By combining ensemble transport with principled reweighting using mixture proposals, we extend weighted variants of the EnKF ([Papadakis et al., 2010; van Leeuwen et al., 2019](#)), improving robustness in nonlinear and non-Gaussian settings while maintaining computational scalability.

3. Notation

Throughout the manuscript we make two standard abuses of notation. First, we do not distinguish between a probability distribution on \mathbb{R}^d and its density with respect to Lebesgue measure: if a random variable x has density p , we write both $x \sim p$ and $p(x)$ for its density at $x \in \mathbb{R}^d$. Second, we reuse the letter p for different probability densities, with the arguments indicating which law is meant; for instance, $p(x)$ denotes the density of x , while $p(y|x)$ denotes the conditional density of y given x .

We write I_d for the $d \times d$ identity matrix, $\text{ran } A$ for the range of a matrix A and \mathbf{S}_{++}^d and \mathbf{S}_+^d for the sets of symmetric positive definite and symmetric positive semidefinite matrices $A \in \mathbb{R}^{d \times d}$, respectively. For $C \in \mathbf{S}_{++}^d$ and $z \in \mathbb{R}^d$ we use the induced norm

$$|z|_C := (z^\top C^{-1} z)^{1/2} = \|C^{-1/2} z\|_2.$$

For integrals over \mathbb{R}^d we use the shorthand

$$\int \psi := \int_{\mathbb{R}^d} \psi(x) \, dx.$$

For random vectors x in \mathbb{R}^{d_x} , y in \mathbb{R}^{d_y} and z in \mathbb{R}^{d_z} with finite second moments, $\mathbb{E}[x]$ and $\mathbb{V}[x]$ denote expectation and variance of x (we only use $\mathbb{V}[x]$ when $d_x = 1$), while the (cross-)covariance matrices are defined as

$$\text{Cov}[x] := \mathbb{E}[(x - \mathbb{E}[x])(x - \mathbb{E}[x])^\top], \quad \text{Cov}[x, y] := \mathbb{E}[(x - \mathbb{E}[x])(y - \mathbb{E}[y])^\top],$$

with $\text{Cov}[x | z]$, $\text{Cov}[x, y | z]$ denoting the corresponding conditional (cross-)covariances. If $g: \mathbb{R}^d \rightarrow \mathbb{R}$ is integrable under the probability density $p: \mathbb{R}^d \rightarrow \mathbb{R}$, we use the additional notation

$$\mathbb{E}_p[g] := \int p g = \mathbb{E}[g(x)], \quad x \sim p.$$

Given vectors $x^{(i)} \in \mathbb{R}^{d_x}$ and $y^{(i)} \in \mathbb{R}^{d_y}$, $i = 1, \dots, N$, with sample means $\bar{x} := \frac{1}{N} \sum_{i=1}^N x^{(i)}$, $\bar{y} := \frac{1}{N} \sum_{i=1}^N y^{(i)}$, we define the empirical (cross-)covariance by

$$\text{Cov}^{\text{emp}}[(x^{(i)})_{i=1}^N, (y^{(i)})_{i=1}^N] := \frac{1}{N-1} \sum_{i=1}^N (x^{(i)} - \bar{x})(y^{(i)} - \bar{y})^\top \in \mathbb{R}^{d_x \times d_y},$$

and abbreviate $\text{Cov}^{\text{emp}}[(x^{(i)})_{i=1}^N] := \text{Cov}^{\text{emp}}[(x^{(i)})_{i=1}^N, (x^{(i)})_{i=1}^N]$.

4. Importance Reweighting with Mixture Targets and Proposals

When estimating expected values $I = \mathbb{E}_p[g]$, but direct sampling from the target distribution p is not possible, importance sampling (IS) provides a strategy to instead sample from a different *proposal* distribution q with $p \ll q$, and to compensate for the discrepancy between p and q by employing importance weights $w(x) = p(x)/q(x)$. This leads to the IS estimator

$$\hat{I}_{\text{IS}} = \frac{1}{N} \sum_{i=1}^N w(x^{(i)}) g(x^{(i)}), \quad x^{(i)} \stackrel{\text{i.i.d.}}{\sim} q.$$

In the setting common to Bayesian statistics, where p is only known up to a normalization constant, one employs self-normalized IS (SNIS), where the weights above are renormalized to sum to one (Owen, 2013; Rubinstein and Kroese, 2016).

Multiple importance sampling (MIS) considers a single target p and several proposals $(q_i)_{i=1}^N$, which gives rise to a range of different IS strategies (Veach and Guibas, 1995). Among others, one can employ *random-mixture* sampling, drawing $x^{(i)} \stackrel{\text{i.i.d.}}{\sim} q_{\text{mix}} := N^{-1} \sum_i q_i$, or *deterministic/stratified* sampling, drawing one point from each q_i .

In our setting, both the target and the proposal densities are equally weighted mixtures,

$$p_{\text{mix}} = \frac{1}{N} \sum_{i=1}^N p_i, \quad q_{\text{mix}} = \frac{1}{N} \sum_{i=1}^N q_i. \tag{4.1}$$

This section focuses on deriving and comparing several different unbiased importance sampling estimators based on the following heuristic approximation of integrals by empirical averages:

$$\mathbb{E}_{p_{\text{mix}}} [g] = \int p_{\text{mix}} g = N^{-1} \sum_{i=1}^N \int \check{p}_i g = N^{-1} \sum_{i=1}^N \int \frac{\check{p}_i g}{\check{q}_i} \check{q}_i \approx N^{-1} \sum_{i=1}^N \frac{\check{p}_i g}{\check{q}_i} (x_i), \quad (4.2)$$

where either $\check{p}_i = p_i$ or $\check{p}_i = p_{\text{mix}}$, either $\check{q}_i = q_i$ or $\check{q}_i = q_{\text{mix}}$, and, for each i , $x_i \sim \check{q}_i$ is an independent draw from \check{q}_i . This leads to the following five unbiased importance sampling estimators (first letter stands for individual (I) or mixture (M) target \check{p}_i , the second one for individual or mixture proposal \check{q}_i)

$$\begin{aligned} \text{II}(g) &:= \frac{1}{N} \sum_{i=1}^N \frac{p_i(x_i)}{q_i(x_i)} g(x_i), & \text{MI}(g) &:= \frac{1}{N} \sum_{i=1}^N \frac{p_{\text{mix}}(x_i)}{q_i(x_i)} g(x_i), & x_i &\stackrel{\text{indep.}}{\sim} q_i; \\ \text{IM}(g) &:= \frac{1}{N} \sum_{i=1}^N \frac{p_i(x_i)}{q_{\text{mix}}(x_i)} g(x_i), & \text{MM}(g) &:= \frac{1}{N} \sum_{i=1}^N \frac{p_{\text{mix}}(x_i)}{q_{\text{mix}}(x_i)} g(x_i), & x_i &\stackrel{\text{i.i.d.}}{\sim} q_{\text{mix}}; \\ \text{MM}^{\text{str}}(g) &:= \frac{1}{N} \sum_{i=1}^N \frac{p_{\text{mix}}(x_i)}{q_{\text{mix}}(x_i)} g(x_i), & x_i &\stackrel{\text{indep.}}{\sim} q_i. \end{aligned}$$

The last estimator, MM^{str} , differs from MM in the way the points x_i are drawn from q_{mix} —instead of i.i.d. samples from q_{mix} , one sample is chosen from each component. This procedure is referred to as stratified, balanced or deterministic sampling, and the resulting estimator MM^{str} is also unbiased with a provably smaller variance than MM (Rubinstein and Kroese, 2016, Proposition 5.5.1).

Theorem 4.1. *Let $p_i, q_i: \mathbb{R}^d \rightarrow \mathbb{R}$, $i = 1, \dots, N$ be probability density functions, let $p_{\text{mix}}, q_{\text{mix}}$ given by (4.1) and let $g \in L^2(p_{\text{mix}})$. Assume that $p_{\text{mix}} \ll q_i$ for each $i = 1, \dots, N$. Then $\text{II}(g), \text{MI}(g), \text{IM}(g), \text{MM}(g), \text{MM}^{\text{str}}(g)$ are unbiased estimators of $I = \mathbb{E}_{p_{\text{mix}}} [g]$ satisfying*

$$\mathbb{V}[\text{MM}^{\text{str}}(g)] \leq \mathbb{V}[\text{MM}(g)] \leq \min(\mathbb{V}[\text{IM}(g)], \mathbb{V}[\text{MI}(g)]). \quad (4.3)$$

Moreover, apart from (4.3), there is no further general variance inequality relating these five estimators.

Proof. The unbiasedness of the estimators is straightforward (cf. (4.2)). The first inequality in (4.3) is an application of the law of total variance,

$$\mathbb{V}[\text{MM}(g)] = \mathbb{V}[\text{MM}^{\text{str}}(g)] + \frac{1}{N} \mathbb{V}_{j \sim \text{Unif}(\{1, \dots, N\})} \left[\mathbb{E}_{q_j} \left[\frac{p_{\text{mix}}}{q_{\text{mix}}} g \right] \right],$$

for details see (Rubinstein and Kroese, 2016, Proposition 5.5.1).

In order to compare $\text{MI}(g)$ with $\text{MM}(g)$, consider their variances:

$$\mathbb{V}[\text{MI}(g)] = \frac{1}{N^2} \sum_{i=1}^N \left(\mathbb{E}_{q_i} \left[\left(\frac{p_{\text{mix}} g}{q_i} \right)^2 \right] - I^2 \right), \quad \mathbb{V}[\text{MM}(g)] = \frac{1}{N} \left(\mathbb{E}_{q_{\text{mix}}} \left[\left(\frac{p_{\text{mix}} g}{q_{\text{mix}}} \right)^2 \right] - I^2 \right).$$

Then, $\mathbb{V}[\text{MM}(g)] \leq \mathbb{V}[\text{MI}(g)]$ follows from

$$\mathbb{E}_{q_{\text{mix}}} \left[\left(\frac{p_{\text{mix}} g}{q_{\text{mix}}} \right)^2 \right] = \frac{1}{N} \int \frac{(\sum_i p_{\text{mix}} g)^2}{\sum_i q_i} \leq \frac{1}{N} \int \sum_{i=1}^N \frac{(p_{\text{mix}} g)^2}{q_i} = \frac{1}{N} \sum_{i=1}^N \mathbb{E}_{q_i} \left[\left(\frac{p_{\text{mix}} g}{q_i} \right)^2 \right],$$

where the inequality above is a pointwise application of Titu's lemma (also known as Cauchy–Schwarz inequality in Engel form or Sedrakyan's inequality):

$$\frac{(\sum_i a_i)^2}{\sum_i b_i} \leq \sum_i \frac{a_i^2}{b_i} \quad \text{whenever } a_i \in \mathbb{R}, b_i > 0 \text{ for all } i. \quad (4.4)$$

In order to compare $\text{MM}(g)$ with $\text{IM}(g)$, we denote $I_i := \mathbb{E}_{p_i}[g] = \int p_i g$ and derive

$$\begin{aligned} \mathbb{V}[\text{MM}(g)] &= \frac{1}{N} \mathbb{E}_{q_{\text{mix}}} \left[\left(\frac{p_{\text{mix}} g}{q_{\text{mix}}} - I \right)^2 \right] \\ &= \frac{1}{N} \mathbb{E}_{q_{\text{mix}}} \left[\left(\frac{1}{N} \sum_{i=1}^N \frac{p_i g}{q_{\text{mix}}} - I_i \right)^2 \right] \\ &\leq \frac{1}{N} \mathbb{E}_{q_{\text{mix}}} \left[\frac{1}{N} \sum_{i=1}^N \left(\frac{p_i g}{q_{\text{mix}}} - I_i \right)^2 \right] \\ &= \frac{1}{N^2} \sum_{i=1}^N \mathbb{E}_{q_{\text{mix}}} \left[\left(\frac{p_i g}{q_{\text{mix}}} - I_i \right)^2 \right] \\ &= \mathbb{V}[\text{IM}(g)], \end{aligned}$$

where the inequality is a (pointwise) application of Jensen's inequality to the convex function $x \mapsto x^2$. The discrete counterexamples¹ collected in [Section A](#) show that no additional general ordering between the variances of II , MI , IM , MM and MM^{str} can hold. ■

Remark 4.2. Clearly,

- (i) if all targets coincide, $p_1 = \dots = p_N$, then $\text{II} = \text{MI}$ and $\text{IM} = \text{MM}$;
- (ii) if all proposals coincide, $q_1 = \dots = q_N$, then $\text{II} = \text{IM}$ and $\text{MI} = \text{MM}$;
- (iii) if each proposal exactly matches its target, $q_i = p_i$ for all i , then $\text{II} = \text{MI} = \text{MM}^{\text{str}}$ reduce to the stratified plain Monte–Carlo estimator (without importance reweighting).

Case (i) corresponds to classical *multiple importance sampling* (MIS) with a single target p and multiple proposals $(q_i)_{i=1}^N$: here $\text{II} = \text{MI}$ is the standard naïve multi-proposal estimator, while $\text{IM} = \text{MM}$ and MM^{str} are the (random vs. stratified) mixture-sampling variants with weights p/q_{mix} ([Owen and Zhou, 2000](#); [Owen, 2013](#); [Veach and Guibas, 1995](#)). Our framework additionally allows *mixture targets*, and these results extend partially to the case of *unequal mixture weights* and *unequal per-component sample counts*, both of which are common in MIS.

Remark 4.3. In this section we have assumed normalized target densities, so all importance sampling (IS) schemes are used in their standard form and yield unbiased estimators. In our later applications the targets are Bayesian posteriors known only up to a normalizing constant, so we employ the corresponding self-normalized IS estimators. These are generally biased but asymptotically unbiased and consistent, so the variance comparisons in this section should be understood as describing the large-sample behavior of the corresponding self-normalized estimators. Further comparisons of the self-normalized schemes in terms of their weights are given in [Theorem 6.2](#) in the context of filtering.

¹For simplicity these counterexamples are given on the discrete two-point space $X = \{0, 1\}$, but they can be embedded without difficulty into the setting of [Theorem 4.1](#).

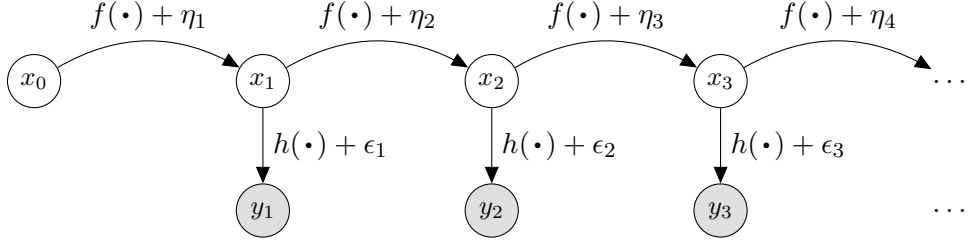


Figure 5.1: State-space model with underlying dynamics (top row) and observations (bottom row).

5. The Filtering Problem: BPF and EnKF

We consider the filtering problem for a state-space model, where we observe a sequence of measurements $(y_t)_{t=1}^T$ in \mathbb{R}^m generated by an underlying, unobserved state sequence $(x_t)_{t=0}^T$ in \mathbb{R}^d . For $t = 1, \dots, T$, the dynamics and observation models are given by:

$$x_t = f(x_{t-1}) + \eta_t, \quad \eta_t \sim \mathcal{N}(0, Q), \quad (5.1)$$

$$y_t = h(x_t) + \epsilon_t, \quad \epsilon_t \sim \mathcal{N}(0, R), \quad (5.2)$$

as illustrated in [Figure 5.1](#), where we assume $x_0 \sim p_0$ and the i.i.d. noise sequences (η_t) and (ϵ_t) to be independent, and $Q \in \mathbf{S}_{++}^d$ and $R \in \mathbf{S}_{++}^m$ to be symmetric and strictly positive definite covariance matrices. Here, $f: \mathbb{R}^d \rightarrow \mathbb{R}^d$ drives the underlying dynamics, and $h: \mathbb{R}^d \rightarrow \mathbb{R}^m$ is the observation function. We assume both f and h to be continuous and we often write H in place of h whenever it is linear, as is common in the literature. We denote by $Y_t := (y_1, \dots, y_t)$ the observed data up to time $t \in \mathbb{N}$ and introduce the conditional distributions

$$\pi_t^{\text{prior}} = p(x_t | Y_{t-1}), \quad p_t^{\text{post}} = p(x_t | Y_t), \quad t \in \mathbb{N}. \quad (5.3)$$

The objective of the filtering problem is to determine the *filtering distribution* p_t^{post} , which is typically intractable in high-dimensional systems. Instead of maintaining an explicit density function, it is usually approximated using a finite set of (possibly weighted) samples, or *particles*, $(x_t^{(i)})_{i=1}^N$ forming an ensemble representation in the Monte Carlo sense. This ensemble is evolved through time, with prediction and update steps ensuring that it remains a reasonable approximation of the true posterior:

1. **Prediction Step:** Propagate the distribution forward using the system dynamics.
2. **Analysis Step:** Incorporate the new observation using Bayes' theorem to update the distribution.

In the prediction step, propagating the particles is straightforward: simply apply the dynamics function f and add independent noise to each particle:

$$\hat{x}_t^{(i)} = f(x_{t-1}^{(i)}) + \eta_t^{(i)}, \quad \eta_t^{(i)} \sim \mathcal{N}(0, Q). \quad (5.4)$$

This step produces an ensemble of particles $(\hat{x}_t^{(i)})_{i=1}^N$ that represents the prior distribution π_t^{prior} at the next time step. For the update (or analysis) step, where the observation y_t is used to adjust the particle ensemble to reflect the posterior distribution p_t^{post} , the methodologies differ based on the filtering approach. In this paper, we concentrate on two common methods, the bootstrap particle filter (BPF; [Gordon et al. 1993](#)) and the ensemble Kalman filter (EnKF; [Evensen 1994, 2003](#)), summarized in [Algorithm 1](#):

Algorithm 1 Bootstrap Particle Filter (BPF) and Ensemble Kalman Filter (EnKF)

- 1: **Inputs:** ensemble size N , horizon T , prior p_0 , dynamics f , observation function h , covariances Q, R , observations $(y_t)_{t=1}^T$, choice of method $\in \{\text{BPF, EnKF}\}$.
- 2: **Initialize:** $x_0^{(i)} \stackrel{\text{i.i.d.}}{\sim} p_0$.
- 3: **for** $t = 1$ to T **do**
- 4: **Prediction step:** Propagate each particle forward via (5.4) $\rightsquigarrow (\hat{x}_t^{(i)})_{i=1}^N$.
- 5: **Kalman gain estimation (not required for BPF):**
 - If h is nonlinear, compute $K_t = \hat{C}_t^{xy}(\hat{C}_t^y)^{-1}$ via (5.9).
 - If h is linear, compute $K_t = K_{p,t}$ via (5.12).
- 6: **Analysis step:**
 - For BPF set $\tilde{x}_t^{(i)} = \hat{x}_t^{(i)}$.
 - For EnKF update each particle via (5.6) $\rightsquigarrow (\tilde{x}_t^{(i)})_{i=1}^N$.
- 7: **Weights and Resampling:**
 - For BPF set $w_t^{(i)} \propto p(y_t | \tilde{x}_t^{(i)})$ and normalize; resample via (5.5) to get $(x_t^{(i)})_{i=1}^N$.
 - For EnKF set $x_t^{(i)} = \tilde{x}_t^{(i)}$ (no resampling).
- 8: **end for**

Bootstrap Particle Filter (BPF). Each particle² $\tilde{x}_t^{(i)} := \hat{x}_t^{(i)}$ is reweighted according to its likelihood with respect to the new observation, $w_t^{(i)} \propto p(y_t | \tilde{x}_t^{(i)})$ with $\sum_{i=1}^N w_t^{(i)} = 1$, followed by a systematic³ resampling step (Doucet and Johansen, 2011, Section 3.4) to mitigate weight degeneracy, that is, a new set of N equally weighted particles $(x_t^{(i)})_{i=1}^N$ is drawn from the distribution $\sum_{i=1}^N w_t^{(i)} \delta_{\tilde{x}_t^{(i)}}$ defined by the current set of weighted particles: Draw $u_1 \sim \text{Unif}(0, N^{-1})$ and set $u_i := u_1 + (i-1)/N$ for $i = 1, \dots, N$ as well as

$$x_t^{(i)} = \tilde{x}_t^{(\text{ind}(i))}, \quad \text{ind}(i) = \min \left\{ j \in \{1, \dots, N\} : \sum_{\ell=1}^j w_t^{(\ell)} \geq u_i \right\}. \quad (5.5)$$

Ensemble Kalman Filter (EnKF). The forecasted (prior) particles $(\hat{x}_t^{(i)})_{i=1}^N$ are shifted based on the *Kalman gain* K_t , transporting them to the analysis (posterior) states $\tilde{x}_t^{(i)}$ which approximate the posterior without explicitly reweighting,

$$\tilde{x}_t^{(i)} = \hat{x}_t^{(i)} + K_t(y_t + \tilde{\epsilon}_t^{(i)} - h(\hat{x}_t^{(i)})), \quad \tilde{\epsilon}_t^{(i)} \stackrel{\text{i.i.d.}}{\sim} \mathcal{N}(0, R) \quad (5.6)$$

Here, we adopted the standard stochastic EnKF with perturbed observations, which preserves ensemble spread by adding artificial observation noise $(\tilde{\epsilon}_t^{(i)})_{i=1}^N$ (e.g. Evensen, 1994, 2003), while the so-called Kalman gain K_t estimates $\text{Cov}[x_t, y_t | Y_{t-1}] \text{Cov}[y_t | Y_{t-1}]^{-1}$ from ensemble covariances, see Section 5.1 below. Unless a resampling or mutation step follows, we set $x_t^{(i)} := \tilde{x}_t^{(i)}$.

EnKF with Importance Weights. The EnKF avoids explicit reweighting by transporting particles directly to regions of higher posterior probability. This makes it computationally efficient and scalable to high-dimensional settings. However, due to the derivation of the EnKF from

²To align notation with the EnKF, we simply relabel the BPF forecast particles as $\tilde{x}_t^{(i)}$. This is entirely unnecessary for the BPF itself, but it makes the resampling step (5.5) identical across the BPF and the (weighted) EnKF variants discussed later. No algorithmic change is implied.

³We use *systematic* rather than *multinomial* resampling because, conditional on the weights, it remains unbiased but has lower conditional variance (Doucet and Johansen, 2011, Section 3.4).

the Gaussian conditioning formula, it is only consistent in the case of normally distributed x_0 and *linear* dynamics f and the observation function h (and only if the noise η_t and ε_t are normally distributed). In most other cases EnKF introduces a bias, because it ignores non-Gaussian features of the forecast distribution and the observation. One remedy to avoid this bias is by establishing the actual distribution that the points $\tilde{x}_t^{(i)}$ are drawn from and using it as the proposal distribution in a subsequent importance reweighting step, as for the well-known weighted EnKF (WEnKF; Papadakis et al. 2010; van Leeuwen et al. 2019). This can be viewed as combining EnKF with BPF and thereby getting the best from both worlds: The ability of EnKF to transport/shift points to meaningful locations and the consistency of BPF. It turns out that there is more than one option to establish the proposal distribution in a consistent and unbiased way, which is the topic of this paper. In fact, the update rule (5.6) implies:

Proposition 5.1 (conditional laws as proposals). *Fix $t \in \mathbb{N}$ and assume $\tilde{\varepsilon}_t^{(i)}$ are independent of $(\hat{x}_t^{(j)})_{j=1}^N$ and of the process and observation noises in (5.1), (5.2) and (5.4).*

(a) **Conditioning on current particles.** *If K_t is a function solely of the forecast ensemble $(\hat{x}_t^{(j)})_{j=1}^N$, then, for each $i = 1, \dots, N$,*

$$q_{c,t}^{(i)} := p(\tilde{x}_t^{(i)} \mid (\hat{x}_t^{(j)})_{j=1}^N) = \mathcal{N}(m_{c,t}^{(i)}, \Sigma_{c,t}), \quad m_{c,t}^{(i)} = \hat{x}_t^{(i)} + K_t(y_t - h(\hat{x}_t^{(i)})), \quad \Sigma_{c,t} = K_t R K_t^\top. \quad (5.7)$$

(b) **Conditioning on previous particles for linear observations.** *If $h(x) = Hx$ is linear and K_t is a function solely of $(x_{t-1}^{(j)})_{j=1}^N$ (independent of the forecast noises $\eta_t^{(j)}$), then, for each $i = 1, \dots, N$,*

$$q_{p,t}^{(i)} := p(\tilde{x}_t^{(i)} \mid (x_{t-1}^{(j)})_{j=1}^N) = \mathcal{N}(m_{p,t}^{(i)}, \Sigma_{p,t}), \quad m_{p,t}^{(i)} = f(x_{t-1}^{(i)}) + K_t(y_t - Hf(x_{t-1}^{(i)})), \quad \Sigma_{p,t} = (\text{Id} - K_t H) Q (\text{Id} - K_t H)^\top + K_t R K_t^\top. \quad (5.8)$$

Proof. For (a), note that in (5.6) the only randomness conditional on $(\hat{x}_t^{(j)})_{j=1}^N$ and K_t is $\tilde{\varepsilon}_t^{(i)}$, linearly mapped by K_t , resulting in the stated Gaussian distribution. For (b), plugging $\hat{x}_t^{(i)} = f(x_{t-1}^{(i)}) + \eta_t^{(i)}$ into (5.6) yields

$$\begin{aligned} \tilde{x}_t^{(i)} &= f(x_{t-1}^{(i)}) + \eta_t^{(i)} + K_t(y_t + \tilde{\varepsilon}_t^{(i)} - Hf(x_{t-1}^{(i)}) - H\eta_t^{(i)}) \\ &= \left[f(x_{t-1}^{(i)}) + K_t(y_t - Hf(x_{t-1}^{(i)})) \right] + \left[(I - K_t H)\eta_t^{(i)} + K_t \tilde{\varepsilon}_t^{(i)} \right]. \end{aligned}$$

yielding the stated mean and covariance (where we used independence of $\eta_t^{(i)}$ and $\tilde{\varepsilon}_t^{(i)}$). ■

For linear observation functions h , the formulas for $q_{c,t}^{(i)}$ and $q_{p,t}^{(i)}$ appear in (Frei and Künsch, 2013b; Papadakis et al., 2010; van Leeuwen et al., 2019); Theorem 5.1 unifies them and makes explicit the exact conditions under which they hold—most notably the permissible construction of K_t from appropriate ensembles and the linearity requirement for h in the previous-ensemble case.

As we will discuss in detail in Section 6, apart from distinguishing between conditioning on current or previous particles, we can also work with individual or mixture proposals, as well as with individual or mixture targets, allowing for more variety in performing importance reweighting, cf. Section 4. In this sense, our work can be seen as an extension of WEnKF, with an additional contribution of incorporating TQMC into this procedure (see Section 7).

Remark 5.2 (square-root/ETKF variants). Deterministic/square-root EnKF updates avoid $\tilde{\epsilon}_t^{(i)}$ and adjust ensemble anomalies directly. Then the conditional proposal is singular (supported on an affine image of the forecast ensemble), which is less convenient for IS. Our methodology therefore uses the stochastic EnKF throughout.

5.1. Estimating the Kalman Gain

Let us discuss certain issues concerning the computation of the Kalman gain K_t , which, as mentioned above, attempts to approximate $\text{Cov}[x_t, y_t | Y_{t-1}] \text{Cov}[y_t | Y_{t-1}]^{-1}$. Since

$$\text{Cov}[x_t, y_t | Y_{t-1}] = \text{Cov}[x_t, h(x_t) | Y_{t-1}], \quad \text{Cov}[y_t | Y_{t-1}] = \text{Cov}[h(x_t) | Y_{t-1}] + R,$$

it is both natural and common to estimate these covariances by

$$\hat{C}_t^{xy} = \text{Cov}^{\text{emp}}[(\hat{x}_t^{(i)})_{i=1}^N, (h(\hat{x}_t^{(i)}))_{i=1}^N], \quad \hat{C}_t^y = \text{Cov}^{\text{emp}}[(h(\hat{x}_t^{(i)}))_{i=1}^N] + R \quad (5.9)$$

and to use the common Kalman gain $K_t = K_t^c$ with

$$K_t^c = \hat{C}_t^{xy} (\hat{C}_t^y)^{-1}. \quad (5.10)$$

For linear $h(x) = Hx$, this Kalman gain reduces to

$$K_t^c = \hat{C}_t^x H^\top (H \hat{C}_t^x H^\top + R)^{-1}, \quad \hat{C}_t^x = \text{Cov}^{\text{emp}}[(\hat{x}_t^{(i)})_{i=1}^N]. \quad (5.11)$$

Interaction issue when conditioning on previous particles. If $K_t = \hat{C}_t^{xy} (\hat{C}_t^y)^{-1}$ is computed from the *forecast* ensemble $(\hat{x}_t^{(i)})_{i=1}^N$ via (5.10) or (5.11), it depends on the forecast noises $\eta_t^{(i)}$ and is therefore *correlated* with the randomness in the analysis update (5.6). Moreover, as noted by [Papadakis et al. \(2010, Section 3\)](#), this dependence on the forecast ensemble induces *interaction* between particles, so the Gaussian formula for $q_{p,t}^{(i)}$ in [Theorem 5.1\(b\)](#) is only a mean-field approximation; the true conditional law $q_{p,t}^{(i)}$ is considerably more complex:

In the establishment of this distribution, we have neglected the dependence on the other particles (which appears through the forecast ensemble covariance) by treating the forecast ensemble covariance as a mean-field variable intrinsic to the system, independent of system realizations—an assumption that holds only asymptotically as the number of particles tends to infinity. ([Papadakis et al., 2010, Section 3](#))

A consistent “previous-ensemble” gain for linear observations. For a linear observation function $h(x) = Hx$ we propose a Kalman gain $K_t = K_t^p$ *independent of the current forecast noises*:

$$K_t^p := \hat{C}_t^{x,p} H^\top (H \hat{C}_t^{x,p} H^\top + R)^{-1}, \quad \hat{C}_t^{x,p} := \text{Cov}^{\text{emp}}[(f(x_{t-1}^{(i)}))_{i=1}^N] + Q, \quad (5.12)$$

where the estimate $\hat{C}_t^{x,p}$ is based on the law of total covariance,

$$\text{Cov}[x_t | Y_{t-1}] = \text{Cov}[f(x_{t-1}) | Y_{t-1}] + Q. \quad (5.13)$$

By construction, K_t^p depends only on $(x_{t-1}^{(i)})_{i=1}^N$, hence, using $K_t = K_t^p$ in (5.6) makes [Theorem 5.1\(b\)](#) exact. Moreover, $\hat{C}_t^{x,p} \rightarrow \text{Cov}[x_t | Y_{t-1}]$ almost surely (a.s.) as $N \rightarrow \infty$ under mild conditions:

Lemma 5.3 (strong consistency). *If $(x_{t-1}^{(i)})_{i=1}^N \stackrel{\text{i.i.d.}}{\sim} p(x_{t-1} | Y_{t-1})$ and $\mathbb{E}[\|f(x_{t-1})\|^2] < \infty$, then*

$$\hat{C}_t^{x,p} \rightarrow \text{Cov}[x_t | Y_{t-1}] \quad \text{a.s. as } N \rightarrow \infty.$$

Proof. Let $Z_i = f(x_{t-1}^{(i)})$. By the (conditional) strong law of large numbers, $\bar{Z}_N \rightarrow \mathbb{E}[Z_1 | Y_{t-1}]$ and $N^{-1} \sum_{i=1}^N Z_i Z_i^\top \rightarrow \mathbb{E}[Z_1 Z_1^\top | Y_{t-1}]$ a.s., hence $\text{Cov}^{\text{emp}}[(Z_i)_{i=1}^N] \rightarrow \text{Cov}[Z_1 | Y_{t-1}]$ a.s. Since η_t is independent of x_{t-1} , the law of total covariance (5.13) proves the claim. \blacksquare

Practically, the estimate $\hat{C}_t^{x,p}$ typically yields a stabler gain (less sampling noise): compared with the forecast-ensemble covariance $\hat{C}_t^x = \text{Cov}^{\text{emp}}[(\hat{x}_t^{(i)})]$ with $\hat{x}_t^{(i)} = f(x_{t-1}^{(i)}) + \eta_t^{(i)}$, the estimator $\hat{C}_t^{x,p}$ uses the known Q exactly and avoids sampling the additive-noise term and random cross-terms, thereby reducing the variance of the covariance estimate. For this reason, whenever h is linear, we recommend using the previous-ensemble gain K_t^p from (5.12) for the EnKF update—even if the proposal in the subsequent IS step is the current-ensemble law $q_{c,t}^{(i)}$.

A consistent “current-ensemble” gain for nonlinear observations. The construction above works only for linear observation functions $h(x) = Hx$. For nonlinear h it is unclear how to obtain consistent estimators $\hat{C}_t^{xy} \approx \text{Cov}[x_t, y_t | Y_{t-1}]$ and $\hat{C}_t^y \approx \text{Cov}[y_t | Y_{t-1}]$ that depend solely on $(x_{t-1}^{(j)})_{j=1}^N$ so that Theorem 5.1(b) would apply. Even if such estimators were available, the conditional law $q_{p,t}^{(i)} = p(\tilde{x}_t^{(i)} | (x_{t-1}^{(j)})_{j=1}^N)$ in general does not admit a closed-form expression, since the composition $h(f(x_{t-1}^{(i)}) + \eta_t^{(i)})$ does not admit a decomposition similar to the one in the proof of Theorem 5.1(b), making an IS step based on $q_{p,t}^{(i)}$ unclear or infeasible without further approximations.

By contrast, the *current-ensemble* gain $K_t^c = \hat{C}_t^{xy}(\hat{C}_t^y)^{-1}$ from (5.10) is well defined for general h and, on the full forecast ensemble $(\hat{x}_t^{(j)})_{j=1}^N$, yields a closed-form Gaussian proposal $q_{c,t}^{(i)} = p(\tilde{x}_t^{(i)} | (\hat{x}_t^{(j)})_{j=1}^N)$ with mean and covariance as in Theorem 5.1(a). One of our contributions is to exploit this current-ensemble proposal $q_{c,t}^{(i)}$ in the reweighting strategies developed in Section 6.

Remark 5.4. In summary, both conditionals $q_{c,t}^{(i)}$ and $q_{p,t}^{(i)}$ from Theorem 5.1 can serve as proposal distributions for importance sampling and may be paired with either gain K_t^c or K_t^p . Their applicability comes with the following notes:

- **Linear-only:** K_t^p and the closed-form Gaussian expression for $q_{p,t}^{(i)}$ are defined only for linear observation functions $h(x) = Hx$.
- **General but noisier:** K_t^c applies to general (possibly nonlinear) h , but its empirical construction is typically less stable.
- **WEKF caveat:** Combining $q_{p,t}^{(i)}$ with K_t^c (the choice made in WEKF) violates the assumptions of Theorem 5.1(b); the Gaussian formula (5.8) should then be viewed as an approximation (Papadakis et al., 2010, Sec. 3).
- **Degeneracy of $q_{c,t}^{(i)}$:** The covariance $\Sigma_{c,t}$ becomes singular if $m < d$ or, when K_t^c is used, if $N < d + 1$, which renders $q_{c,t}^{(i)}$ unusable as an IS proposal.

Recommendation. Whenever available (i.e., for linear h), prefer the pair $(q_{p,t}^{(i)}, K_t^p)$. For nonlinear observation functions, fall back to $(q_{c,t}^{(i)}, K_t^c)$, keeping the above restrictions in mind.

6. Importance Sampling Schemes for the Ensemble Kalman Filter

In the EnKF framework, the forecast particles $\hat{x}_t^{(i)}$ and the updated particles $\tilde{x}_t^{(i)}$ can be viewed as stratified (or balanced/deterministic, see Rubinstein and Kroese 2016, Section 5.5) samples

from the mixtures

$$\pi_t^{\text{mix}} = \frac{1}{N} \sum_{i=1}^N \pi_t^{(i)}, \quad \pi_t^{(i)} := \mathcal{N}(f(x_{t-1}^{(i)}), Q), \quad \hat{x}_t^{(i)} \stackrel{\text{indep.}}{\sim} \pi_t^{(i)}, \quad (6.1)$$

$$q_t^{\text{mix}} = \frac{1}{N} \sum_{i=1}^N q_t^{(i)}, \quad q_t^{(i)} = \mathcal{N}(m_t^{(i)}, \Sigma_t), \quad \tilde{x}_t^{(i)} \stackrel{\text{indep.}}{\sim} q_t^{(i)}, \quad (6.2)$$

respectively, where $m_t^{(i)}$ and Σ_t are specified in (5.7) and (5.8) below. That is, both the approximate prior distribution $\pi_t^{\text{mix}} \approx \pi_t^{\text{prior}}$ (van Leeuwen et al., 2019, Equation (26)) and the proposal distribution q_t^{mix} (Frei and Künsch, 2013b, Equation (1)) are Gaussian mixtures. It follows that the (approximate and unnormalized) posterior/target is again a mixture distribution:

$$p_t^{\text{mix}} = \ell_t \pi_t^{\text{mix}} = \frac{1}{N} \sum_{i=1}^N p_t^{(i)}, \quad p_t^{(i)} = \ell_t \pi_t^{(i)}, \quad (6.3)$$

where, for $t \in \mathbb{N}$,

$$\ell_t(x) := \exp(-\frac{1}{2}|y_t - h(x)|_R^2) \in (0, 1], \quad x \in \mathbb{R}^d, \quad (6.4)$$

denotes the (unnormalized) likelihood given observation y_t . As we are working with *stratified* proposal samples $\tilde{x}_t^{(i)} \stackrel{\text{indep.}}{\sim} q_t^{(i)}$, the self-normalized versions of the estimators **II**, **MI** and **MM^{str}** from Section 4 are applicable.⁴ This way the EnKF update (5.6) remains identical across all three strategies, the only difference lies in the *interpretation*—each particle can either be viewed as an independent sample from $q_t^{(i)}$ or, collectively, as a *stratified* sampling from q_t^{mix} .

In addition to distinguishing between individual and mixture reweighting, there are at least two options to establish the individual proposals $q_t^{(i)} = \mathcal{N}(m_t^{(i)}, \Sigma_t)$, as has been established in Theorem 5.1: One can either condition on the current forecast ensemble $(\hat{x}_t^{(j)})_{j=1}^N$ via (5.7), or the previous ensemble $(x_{t-1}^{(j)})_{j=1}^N$ via (5.8),

$$q_t^{(i)} = q_{c,t}^{(i)} = \mathcal{N}(m_{c,t}^{(i)}, \Sigma_{c,t}) \quad \text{or} \quad q_t^{(i)} = q_{p,t}^{(i)} = \mathcal{N}(m_{p,t}^{(i)}, \Sigma_{p,t}).$$

Consequently, this results in $3 \times 2 = 6$ different self-normalized importance sampling strategies for p_t^{post} of the form

$$p_t^{\text{post}} \approx \sum_{i=1}^N w_t^{(i)} \delta_{\tilde{x}_t^{(i)}}, \quad w_t^{(i)} = \frac{v_t^{(i)}}{\sum_j v_t^{(j)}}, \quad v_t^{(i)} = \frac{\check{p}_t^{(i)}}{\check{q}_t^{(i)}}(\tilde{x}_t^{(i)}), \quad (6.5)$$

summarized in Table 6.1 and Algorithm 2 and denoted by

$$\text{II}_c, \quad \text{MI}_c, \quad \text{MM}_c^{\text{str}}, \quad \text{II}_p, \quad \text{MI}_p, \quad \text{MM}_p^{\text{str}},$$

where

- the first letter corresponds to the choice of $\check{p}_t^{(i)}$:
I for “individual”, $\check{p}_t^{(i)} = p_t^{(i)}$, or M for “mixture”, $\check{p}_t^{(i)} = p_t^{\text{mix}}$;

⁴In principle, one could also use **IM** and **MM** by drawing proposals i.i.d. from q_t^{mix} instead of stratified from $(q_t^{(i)})_{i=1}^N$. This would replace the EnKF’s balanced sampling with i.i.d. sampling and thus alter the algorithm; here we keep the EnKF prediction and update steps unchanged. A mixture-sampling analogue of **MM** will be discussed in Section 7.

Algorithm 2 Importance Sampling Schemes for the Ensemble Kalman Filter

- 1: **Inputs:** ensemble size N , horizon T , prior p_0 , dynamics f , observation function h , covariances Q, R , observations $(y_t)_{t=1}^T$, choice of IS scheme $\in \{\text{II}_c, \text{MI}_c, \text{MM}_c^{\text{str}}, \text{II}_p, \text{MI}_p, \text{MM}_p^{\text{str}}\}$ (p -schemes require linear h).
- 2: **Initialize:** Sample $x_0^{(i)} \stackrel{\text{i.i.d.}}{\sim} p_0$.
- 3: **for** $t = 1$ to T **do**
- 4: **Prediction step:** Propagate each particle forward via (5.4) $\rightsquigarrow (\hat{x}_t^{(i)})_{i=1}^N$.
- 5: **Kalman gain estimation:**
 - If h is nonlinear, compute $K_t = K_t^c$ via (5.10).
 - If h is linear, compute $K_t = K_t^p$ via (5.12).
- 6: **Build targets and proposals:**
 - Define $p_t^{(i)} = \ell_t \pi_t^{(i)}$, where $\pi_t^{(i)} = \mathcal{N}(f(x_{t-1}^{(i)}), Q)$, cf. (6.1)–(6.3).
 - Define $q_t^{(i)} = q_{c,t}^{(i)}$ via (5.7) for schemes of the form $\blacksquare\blacksquare_c$.
 - Define $q_t^{(i)} = q_{p,t}^{(i)}$ via (5.8) for schemes of the form $\blacksquare\blacksquare_p$.
 - Define $p_t^{\text{mix}} = N^{-1} \sum_{i=1}^N p_t^{(i)}$ and $q_t^{\text{mix}} = N^{-1} \sum_{i=1}^N q_t^{(i)}$.
- 7: **Analysis step:** update each particle via (5.6) $\rightsquigarrow (\tilde{x}_t^{(i)})_{i=1}^N$.
- 8: **Weights (self-normalized IS):** Set $w_t^{(i)} \propto \frac{\tilde{p}_t^{(i)}}{\tilde{q}_t^{(i)}}(\tilde{x}_t^{(i)})$ and normalize, cf. (6.5), where
 - $\tilde{p}_t^{(i)} = p_t^{(i)}$, $\tilde{q}_t^{(i)} = q_t^{(i)}$ for schemes of the form II_{\blacksquare} ;
 - $\tilde{p}_t^{(i)} = p_t^{\text{mix}}$, $\tilde{q}_t^{(i)} = q_t^{(i)}$ for schemes of the form MI_{\blacksquare} ;
 - $\tilde{p}_t^{(i)} = p_t^{\text{mix}}$, $\tilde{q}_t^{(i)} = q_t^{\text{mix}}$ for schemes of the form $\text{MM}_{\blacksquare}^{\text{str}}$.
- 9: **Resampling:** Choose $x_t^{(i)}$ via (5.5).
- 10: **end for**

- the second letter corresponds to the choice of $\tilde{q}_t^{(i)}$:
- I for “individual”, $\tilde{q}_t^{(i)} = q_t^{(i)}$, or M for “mixture”, $\tilde{q}_t^{(i)} = q_t^{\text{mix}}$;
- the index (c for “current” or p for “previous”) corresponds to the interpretation of the individual proposals $q_t^{(i)}$, cf. (5.7) and (5.8) above.

Note that II_p corresponds to the well-known weighted EnKF (WEnKF; Papadakis et al. 2010; van Leeuwen et al. 2019).

6.1. Generalization to localized EnKF and other filtering algorithms

The reweighting strategy introduced in the previous subsection extends naturally to a broader class of ensemble-based particle filters, including localized variants of the EnKF and related algorithms. The convergence analysis in the subsequent [Section 6.2](#) is formulated within this more general framework.

We continue to work with the state and observation models given by (5.1)–(5.2). At time step t , [Algorithm 2](#) can be viewed as drawing analysis samples $\tilde{x}_t^{(i)} \sim q_t^{(i)}$ from proposals $q_t^{(i)} = q_{c,t}^{(i)}$ or $q_t^{(i)} = q_{p,t}^{(i)}$, as established in [Theorem 5.1](#). These proposals may depend on either $x_{t-1}^{(i)}$ or $\hat{x}_t^{(i)}$ as well as on y_t and, through the Kalman gain K_t , on the full ensembles $(x_{t-1}^{(j)})_{j=1}^N$ or $(\hat{x}_t^{(j)})_{j=1}^N$, cf. (5.7) and (5.8). To encompass localized EnKF and other ensemble-based filters, we replace this specific choice by a generic proposal mechanism of the form

$$q_t^{(i)} = \mathfrak{q}\left(x_{t-1}^{(i)}, \hat{x}_t^{(i)}, \frac{1}{N} \sum_{j=1}^N \delta_{x_{t-1}^{(j)}}, \frac{1}{N} \sum_{j=1}^N \delta_{\hat{x}_t^{(j)}}, y_t\right), \quad (6.6)$$

Table 6.1: The $3 \times 2 = 6$ importance sampling strategies for the EnKF, determined by whether individual or mixture priors, as well as individual or mixture proposals, are used in the reweighting process, and by whether the proposals are conditioned on current or previous particles. Note that II_p corresponds to the well-known weighted EnKF (WEKF; Papadakis et al. 2010; van Leeuwen et al. 2019).

EnKF Reweighting via $p_t^{\text{post}} \approx \sum_{i=1}^N w_t^{(i)} \delta_{\tilde{x}_t^{(i)}}$ $w_t^{(i)} \propto \frac{\tilde{p}_t^{(i)}}{\tilde{q}_t^{(i)}}(\tilde{x}_t^{(i)}),$	■■_c : conditioning on current particles: $m_t^{(i)} = m_{c,t}^{(i)}$ cf. (5.7) $\Sigma_t = \Sigma_{c,t}$	■■_p : conditioning on previous particles: $m_t^{(i)} = m_{p,t}^{(i)}$ cf. (5.8) $\Sigma_t = \Sigma_{p,t}$
$\text{II}_{\blacksquare} : \begin{aligned} \tilde{p}_t^{(i)} &= p_t^{(i)} = \mathcal{N}(f(x_{t-1}^{(i)}), Q) \\ \tilde{q}_t^{(i)} &= q_t^{(i)} = \mathcal{N}(m_t^{(i)}, \Sigma_t) \end{aligned}$	II_c	II_p
$\text{MI}_{\blacksquare} : \begin{aligned} \tilde{p}_t^{(i)} &= p_t^{\text{mix}} = \frac{1}{N} \sum_{i=1}^N p_t^{(i)} \\ \tilde{q}_t^{(i)} &= q_t^{(i)} = \mathcal{N}(m_t^{(i)}, \Sigma_t) \end{aligned}$	MI_c	MI_p
$\text{MM}_{\blacksquare}^{\text{str}} : \begin{aligned} \tilde{p}_t^{(i)} &= p_t^{\text{mix}} = \frac{1}{N} \sum_{i=1}^N p_t^{(i)} \\ \tilde{q}_t^{(i)} &= q_t^{\text{mix}} = \frac{1}{N} \sum_{i=1}^N q_t^{(i)} \end{aligned}$	MM_c^{str}	MM_p^{str}

where $\mathbf{q} : \mathbb{R}^d \times \mathbb{R}^d \times \mathcal{P}(\mathbb{R}^d) \times \mathcal{P}(\mathbb{R}^d) \times \mathbb{R}^m \rightarrow \mathcal{P}_+(\mathbb{R}^d)$ is an arbitrary function that we call *proposal function* and $\mathcal{P}_+(\mathbb{R}^d)$ denotes the set of probability distributions on \mathbb{R}^d with strictly positive probability densities. As before, we define the proposal mixture $q_t^{\text{mix}} := \frac{1}{N} \sum_{i=1}^N q_t^{(i)}$. Using the same three importance sampling strategies as in the previous subsection, but now with the generic *proposal function* \mathbf{q} , we obtain the schemes II_q , MI_q , and MM_q^{str} , which are summarized in [Algorithm 3](#).

Examples of ensemble-based filtering algorithms to which our reweighting framework can be applied include, in addition to the standard stochastic EnKF discussed above, the covariance-localized EnKF (Hamill et al., 2001; Houtekamer and Mitchell, 2001) and EnKF with covariance inflation (Anderson and Anderson, 1999; Whitaker and Hamill, 2012), which are most transparently described in the linear observation case $h(x) = Hx$. In their simplest formulations, both methods amount to modifying the empirical forecast covariance matrix $\hat{C}_t^x = \mathbb{C}^{\text{emp}}[(\hat{x}_t^{(i)})_{i=1}^N]$ via

$$\hat{C}_t^{x,\text{loc}} := L \circ \hat{C}_t^x, \quad \hat{C}_t^{x,\text{infl}} := \delta_t^2 \hat{C}_t^x$$

where L is a localization matrix whose entries depend on the physical distance between state components and \circ denotes the Schur product, while $\delta_t \geq 1$ is an inflation factor. Consequently, these modified covariance matrices enter the Kalman gain $K_t^c = \hat{C}_t^x H^\top (H \hat{C}_t^x H^\top + R)^{-1}$ in (5.11), where \hat{C}_t^x is replaced by either $\hat{C}_t^{x,\text{loc}}$ or $\hat{C}_t^{x,\text{infl}}$, and thus they directly modify the Gaussian proposals in (5.7) and (5.8).

6.2. Convergence Analysis

To demonstrate that importance sampling estimates introduced in [Algorithm 3](#) consistently approximate the posterior distribution in a meaningful way, we introduce the same distance

Algorithm 3 Importance Sampling Schemes in General Framework

- 1: **Inputs:** ensemble size N , horizon T , prior p_0 , dynamics f , observation function h , covariances Q, R , observations $(y_t)_{t=1}^T$, proposal function \mathbf{q} , choice of IS scheme $\in \{\text{II}_{\mathbf{q}}, \text{MI}_{\mathbf{q}}, \text{MM}_{\mathbf{q}}^{\text{str}}\}$
- 2: **Initialize:** Sample $x_0^{(i)} \stackrel{\text{i.i.d.}}{\sim} p_0$.
- 3: **for** $t = 1$ to T **do**
- 4: **Prediction step:** Propagate each particle forward via (5.4) $\rightsquigarrow (\hat{x}_t^{(i)})_{i=1}^N$.
- 5: **Targets** $p_t^{(i)} = \ell_t \cdot \mathcal{N}(f(x_{t-1}^{(i)}), Q)$ and $p_t^{\text{mix}} = N^{-1} \sum_{i=1}^N p_t^{(i)}$.
- 6: **Proposals** $q_t^{(i)} = \mathbf{q}(x_{t-1}^{(i)}, \hat{x}_t^{(i)}, \frac{1}{N} \sum_{j=1}^N \delta_{x_{t-1}^{(j)}}, \frac{1}{N} \sum_{j=1}^N \delta_{\hat{x}_t^{(j)}}, y_t)$ and $q_t^{\text{mix}} = \frac{1}{N} \sum_{i=1}^N q_t^{(i)}$.
- 7: **Analysis step:** Draw independent samples $\tilde{x}_t^{(i)} \sim q_t^{(i)}$, $i = 1, \dots, N$.
- 8: **Weights (self-normalized IS):** Set $w_t^{(i)} \propto \frac{\tilde{p}_t^{(i)}}{q_t^{(i)}}(\tilde{x}_t^{(i)})$ and normalize, cf. (6.5), where
 - $\tilde{p}_t^{(i)} = p_t^{(i)}$, $\tilde{q}_t^{(i)} = q_t^{(i)}$ for $\text{II}_{\mathbf{q}}$;
 - $\tilde{p}_t^{(i)} = p_t^{\text{mix}}$, $\tilde{q}_t^{(i)} = q_t^{(i)}$ for $\text{MI}_{\mathbf{q}}$;
 - $\tilde{p}_t^{(i)} = p_t^{\text{mix}}$, $\tilde{q}_t^{(i)} = q_t^{\text{mix}}$ for $\text{MM}_{\mathbf{q}}^{\text{str}}$.
- 9: **Resampling:** Choose $x_t^{(i)}$ via (5.5).
- 10: **end for**

between random probability density functions as [Sanz-Alonso et al. \(2023, Section 11.3\)](#) did for the analysis of the BPF. For two random probability density functions p, p' on \mathbb{R}^d we define the metric

$$d(p, p') := \sup_{\|g\|_{\infty} \leq 1} \left(\mathbb{E} \left[\left(\int p g - \int p' g \right)^2 \right] \right)^{1/2},$$

where the supremum is taken over all g in the space $C_b(\mathbb{R}^d)$ of continuous bounded functions on \mathbb{R}^d . Note that, in our case, the randomness of the probability densities arises from sampling in the prediction, analysis and resampling step, while we consider the observations $(y_t)_{t=1}^T$ to be fixed.

Theorem 6.1. *Consider the dynamics and observation models given by (5.1)–(5.2) with fixed observations $(y_t)_{t=1}^T \in (\mathbb{R}^m)^T$, continuous observation function $h: \mathbb{R}^d \rightarrow \mathbb{R}^k$ and any of the sampling schemes $\text{II}_{\mathbf{q}}, \text{MI}_{\mathbf{q}}, \text{MM}_{\mathbf{q}}^{\text{str}}$ defined in [Algorithm 3](#) for some proposal function \mathbf{q} of the form (6.6). Further, denote $p_0^{\text{post}} := p_0$, $c_0 := 1$, and, for $t = 1, \dots, T$,*

$$\begin{aligned} c_t &:= 2 \left(\frac{c_{t-1}}{Z_t^{\text{post}}} + \sigma_t + 1 \right) \in [0, \infty], & \sigma_t^2 &:= \mathbb{V} \left[\frac{\tilde{p}_t^{(1)}}{Z_t^{\text{mix}} \tilde{q}_t^{(1)}}(\tilde{x}_t^{(1)}) \right] = \mathbb{V} \left[\frac{v_t^{(1)}}{Z_t^{\text{mix}}} \right] \in [0, \infty], \\ Z_t^{\text{post}} &:= \int \ell_t \pi_t^{\text{prior}}, & Z_t^{\text{mix}} &:= \int p_t^{\text{mix}} = \int \ell_t \pi_t^{\text{mix}}, \end{aligned}$$

where π_t^{prior} , p_t^{post} , π_t^{mix} , p_t^{mix} , $p_t^{(i)}$, ℓ_t and $v_t^{(i)}$ are defined in (5.3), (6.1), (6.3), (6.4) and (6.5), respectively. Then the particle approximation of the filtering distribution p_t^{post} by the ensemble $(x_t^{(i)})_{i=1}^N$ satisfies

$$d_t := d \left(p_t^{\text{post}}, \frac{1}{N} \sum_{i=1}^N \delta_{x_t^{(i)}} \right) \leq \frac{c_t}{\sqrt{N}} \quad \text{for every } t = 0, \dots, T. \quad (6.7)$$

Proof. The claim will be proven by induction, starting with $d_0 \leq N^{-1/2}$ ([Sanz-Alonso et al., 2023, Lemma 11.2](#)). For $t \in \mathbb{N}$, we decompose the error d_t into the approximation error for the

filtering distribution, the (self-normalized) importance sampling error and the resampling error, each of which will be bounded by one of the three lemmas in [Section B: Theorems B.1, B.2, and B.3](#). The proof is then a simple application of the triangle inequality:

$$\begin{aligned}
d_t &\leq \underbrace{d\left(p_t^{\text{post}}, \frac{p_t^{\text{mix}}}{Z_t^{\text{mix}}}\right)}_{\text{approximation error for the filtering distribution}} + \underbrace{d\left(\frac{p_t^{\text{mix}}}{Z_t^{\text{mix}}}, \sum_{i=1}^N w_t^{(i)} \delta_{\tilde{x}_t^{(i)}}\right)}_{\text{SNIS error}} + \underbrace{d\left(\sum_{i=1}^N w_t^{(i)} \delta_{\tilde{x}_t^{(i)}}, \frac{1}{N} \sum_{i=1}^N \delta_{x_t^{(i)}}\right)}_{\text{resampling error}} \\
&\leq \frac{2d_{t-1}}{Z_t^{\text{post}}} + \frac{2\sigma_t + 1}{\sqrt{N}} + \frac{1}{\sqrt{N}} \leq \frac{2}{\sqrt{N}} \left(\frac{c_{t-1}}{Z_t^{\text{post}}} + \sigma_t + 1 \right) = \frac{c_t}{\sqrt{N}}.
\end{aligned}$$

■

The critical condition for [Theorem 6.1](#) to be useful is that the SNIS weights have finite variance, $\sigma_t < \infty$, a standard requirement in importance sampling. Before showing that this assumption can indeed be ensured under suitable conditions ([Theorem 6.3](#)), we first compare the schemes in terms of the variance of their self-normalized weights and show that the mixture–mixture estimators are preferable in this sense. This result can be seen as a complement to [Theorem 4.1](#): here we work in the self-normalized setting and compare weight variance rather than the variance of the estimators themselves, which in general still depends on the integrand g .

Theorem 6.2. *Under the assumptions of [Theorem 6.1](#) and using the notation therein,*

$$\sigma_t \geq \sigma_t^{\text{mix}}, \quad c_t \geq c_t^{\text{mix}},$$

where σ_t^{mix} and c_t^{mix} are the corresponding quantities for the scheme MM_q^{str} .

Proof. Using [\(B.4\)](#) and the notation therein, we obtain in all schemes

$$\begin{aligned}
\sigma_t^2 &= \mathbb{V} \left[\frac{\check{p}_t^{(1)}}{Z_t^{\text{mix}} \check{q}_t^{(1)}} (\tilde{x}_t^{(1)}) \right] \\
&= \mathbb{E} \left[\left(\frac{\check{p}_t^{(1)}}{Z_t^{\text{mix}} \check{q}_t^{(1)}} (\tilde{x}_t^{(1)}) \right)^2 \right] - \mathbb{E} \left[\frac{\check{p}_t^{(1)}}{Z_t^{\text{mix}} \check{q}_t^{(1)}} (\tilde{x}_t^{(1)}) \right]^2 \\
&= \frac{1}{N} \sum_{i=1}^N \mathbb{E} \left[\mathbb{E} \left[\left(\frac{\check{p}_t^{(i)}}{Z_t^{\text{mix}} \check{q}_t^{(i)}} (\tilde{x}_t^{(i)}) \right)^2 \mid \mathcal{F}_t \right] \right] - 1 \\
&= \mathbb{E} \left[\frac{1}{N} \sum_{i=1}^N \int \left(\frac{\check{p}_t^{(i)}}{Z_t^{\text{mix}} \check{q}_t^{(i)}} \right)^2 q_t^{(i)} \right] - 1.
\end{aligned}$$

The scheme MM_q^{str} satisfies $\sigma_t = \sigma_t^{\text{mix}}$ by definition. For the schemes II_q and MI_q we have $\check{q}_t^{(i)} = q_t^{(i)}$, in which case an application of Titu's lemma stated in [\(4.4\)](#) yields

$$\begin{aligned}
\sum_{i=1}^N \int \left(\frac{\check{p}_t^{(i)}}{\check{q}_t^{(i)}} \right)^2 q_t^{(i)} &= \int \sum_{i=1}^N \frac{(\check{p}_t^{(i)})^2}{q_t^{(i)}} \geq \int \frac{1}{N} \frac{(\sum_{i=1}^N \check{p}_t^{(i)})^2}{\sum_{i=1}^N q_t^{(i)}} \\
&= \int \left(\frac{\frac{1}{N} \sum_{i=1}^N \check{p}_t^{(i)}}{\frac{1}{N} \sum_{i=1}^N q_t^{(i)}} \right)^2 \sum_{i=1}^N q_t^{(i)} = \sum_{i=1}^N \int \left(\frac{p_t^{\text{mix}}}{q_t^{\text{mix}}} \right)^2 q_t^{(i)}.
\end{aligned}$$

Therefore,

$$\sigma_t^2 = \mathbb{E} \left[\frac{1}{N} \frac{1}{(Z_t^{\text{mix}})^2} \sum_{i=1}^N \int \left(\frac{\tilde{p}_t^{(i)}}{\tilde{q}_t^{(i)}} \right)^2 q_t^{(i)} \right] - 1 \geq \mathbb{E} \left[\frac{1}{N} \frac{1}{(Z_t^{\text{mix}})^2} \sum_{i=1}^N \int \left(\frac{p_t^{\text{mix}}}{q_t^{\text{mix}}} \right)^2 q_t^{(i)} \right] - 1 = (\sigma_t^{\text{mix}})^2.$$

Since both variances are non-negative, this implies $\sigma_t \geq \sigma_t^{\text{mix}}$. $c_t \geq c_t^{\text{mix}}$ follows directly from the definition. \blacksquare

Next, we show that, for the sampling schemes II_p , MI_p , MM_p^{str} , the finite-variance condition $\sigma_t < \infty$ in [Theorem 6.1](#) is indeed satisfied whenever the observation function h is linear and the model drift f is bounded. Note that we now work in the setting of the weighted EnKF from [Algorithm 2](#) rather than the more general framework of [Algorithm 3](#).

Theorem 6.3. *Let the assumptions of [Theorem 6.1](#) hold and consider the notation therein. In the setting of [Algorithm 2](#), fix $i = 1, \dots, N$ and $t = 1, \dots, T$, assume that the observation function $h(x) = Hx$ is linear, that $K_t = K_t^p = \hat{C}_t^{x,p} H^\top (H \hat{C}_t^{x,p} H^\top + R)^{-1}$ is computed via [\(5.12\)](#), and denote*

$$S := HQH^\top + R \in \mathbf{S}_{++}^m, \quad K := QH^\top S^{-1} \in \mathbb{R}^{d \times m}, \quad \Sigma := Q - KHQ \in \mathbb{R}^{d \times d}.$$

(a) Denoting $\hat{m}_t^{(i)} = f(x_{t-1}^{(i)}) + K(y_t - Hf(x_{t-1}^{(i)}))$, we have $\Sigma \in \mathbf{S}_{++}^d$ and

$$p_t^{(i)} = \left(\frac{\det R}{\det S} \right)^{1/2} \exp \left(-\frac{1}{2} |y_t - Hf(x_{t-1}^{(i)})|_S^2 \right) \cdot \mathcal{N}(\hat{m}_t^{(i)}, \Sigma). \quad (6.8)$$

(b) There exists $u_t^{(i)} \in \mathbb{R}^d$ such that, for each $x \in \mathbb{R}^d$

$$\frac{p_t^{(i)}}{q_{p,t}^{(i)}}(x) \leq \left(\frac{\det \Sigma_{p,t}}{\det Q} \right)^{1/2} \exp \left(-\frac{1}{2} (x - u_t^{(i)})^\top (\Sigma^{-1} - \Sigma_{p,t}^{-1})(x - u_t^{(i)}) \right), \quad (6.9)$$

with equality if $\text{Cov}^{\text{emp}}[(f(x_{t-1}^{(i)}))_{i=1}^N]$ is positive definite and H has full row rank.

(c) For each $x \in \mathbb{R}^d$ and $i = 1, \dots, N$,

$$\frac{p_t^{(i)}}{Z^{\text{mix}} q_{p,t}^{(i)}(x)} \leq \left(\frac{\det \hat{C}_t^{x,p}}{\det Q} \right)^{1/2} \left(\frac{1}{N} \sum_{i=1}^N \exp \left(-\frac{1}{2} |y_t - Hf(x_{t-1}^{(i)})|_S^2 \right) \right)^{-1}. \quad (6.10)$$

Further, for the sampling schemes II_p and MM_p^{str} defined in [Algorithm 2](#), we have $\sigma_t^2 < \infty$ whenever f is bounded.

Proof. The argument proceeds in several steps which are established in [Section C](#). First, we collect several identities among the EnKF matrices in [Theorem C.1](#). Next, using these identities together with a completion-of-squares argument, we prove (a) in [Theorem C.2](#). We then establish (b) in [Theorem C.3](#)—again by completing the square—taking particular care with symmetric matrices that are only positive semidefinite. Finally, [Theorem C.4](#) applies (b) to the targets and proposals in the schemes II_p and MM_p^{str} , yielding (c). \blacksquare

7. TQMC-Enhanced EnKF

As established above, both the approximate prior and the proposal used by the EnKF can be written as Gaussian mixtures:

$$\pi_t^{\text{mix}} = \frac{1}{N} \sum_{i=1}^N \mathcal{N}(f(x_{t-1}^{(i)}), Q), \quad q_t^{\text{mix}} = \frac{1}{N} \sum_{i=1}^N \mathcal{N}(m_t^{(i)}, \Sigma_t),$$

where $(m_t^{(i)}, \Sigma_t)$ are given by (5.7) or (5.8). Instead of drawing i.i.d. (or stratified) samples from these mixtures, we propose to use *transported quasi Monte–Carlo* (TQMC) point sets (Klebanov and Sullivan, 2023): low-discrepancy points in a reference space are pushed forward through an essentially closed-form transport to the mixture distribution. Compared with i.i.d. or stratified sampling, quasi Monte–Carlo (QMC) and randomized quasi Monte–Carlo (RQMC) achieve lower discrepancy and—for sufficiently smooth integrands—provably better mean-squared error rates than $O(N^{-1})$, see, e.g., Owen (2013).

Notation 7.1 (RQMC transport to mixtures). For any Gaussian mixture $p = \sum_{k=1}^K w_k \mathcal{N}(m_k, C_k)$, we write

$$(z^{(i)})_{i=1}^N = \text{TQMC}_N(p)$$

to denote N RQMC points pushed forward by a transport map T_p from the uniform distribution on $(0, 1)^d$ (Klebanov and Sullivan, 2023) so that $(z^{(i)})_{i=1}^N = (T_p(u^{(i)}))_{i=1}^N$ has sampling law p . Throughout our experiments, we choose $(u^{(i)})_{i=1}^N$ to be a scrambled Sobol' sequence (specifically, we employ the Matoušek–Affine–Owen scrambling (Matoušek, 1998; Owen, 1995, 1998)).

In the standard EnKF pipeline, the *resampling step* (5.5) followed by the *prediction step* (5.4) is equivalent to drawing i.i.d. samples from the weighted Gaussian mixture

$$\rho_t^{\text{mix}} := \sum_{i=1}^N w_{t-1}^{(i)} \mathcal{N}(f(\tilde{x}_{t-1}^{(i)}), Q).$$

With TQMC we can skip explicit resampling and directly generate the forecast ensemble as well as the proposals from q_t^{mix} via

$$(\hat{x}_t^{(i)})_{i=1}^N = \text{TQMC}_N(\rho_t^{\text{mix}}), \quad (\tilde{x}_t^{(i)})_{i=1}^N = \text{TQMC}_N(q_t^{\text{mix}}).$$

As before, both $q_{c,t}^{\text{mix}}$ and $q_{p,t}^{\text{mix}}$ can be used for q_t^{mix} , with $q_{p,t}^{\text{mix}}$ limited to *linear* observation functions h , cf. Section 5.1, the only difference being that, in the case $q_t^{\text{mix}} = q_{p,t}^{\text{mix}}$, we are conditioning on a *weighted* ensemble of particles $(x_{t-1}^{(i)}, w_{t-1}^{(i)})_{i=1}^N$ (due to the missing resampling step), and therefore

$$q_{p,t}^{\text{mix}} = \sum_{i=1}^N w_{t-1}^{(i)} q_{p,t}^{(i)}. \quad (7.1)$$

The reweighting can then be performed by MM (with i.i.d. samples replaced by these TQMC points). Note that resampling and prediction in BPF is identical to the one of the weighted EnKF variants, so the same TQMC-enhancement works for the generation of the forecast ensemble in BPF. All of these methods are summarized in Algorithm 4.

Remark 7.2. Note that the transport methodology of Klebanov and Sullivan (2023) is not limited to QMC and RQMC, but can be employed to transport any cubature rule (e.g. sparse grids or digital nets) to a mixture distribution. For a discussion of the computational overhead of TQMC see (Klebanov and Sullivan, 2023).

Algorithm 4 TQMC-Enhanced BPF and (Weighted) EnKF

```

1: Inputs: ensemble size  $N$ , horizon  $T$ , Gaussian or Gaussian-mixture prior  $p_0$ , dynamics  $f$ , observation function  $h$ , covariances  $Q, R$ , observations  $(y_t)_{t=1}^T$ , choice of scheme  $\in \{\text{QMC-BPF}, \text{QMC-EnKF}_c, \text{QMC-MM}_c, \text{QMC-EnKF}_p, \text{QMC-MM}_p\}$  ( $p$ -schemes require linear  $h$ ).
2: Initialize:  $(x_0^{(i)})_{i=1}^N = \text{TQMC}_N(p_0)$  and set  $w_0^{(i)} = \frac{1}{N}$  for all  $i = 1, \dots, N$ .
3: for  $t = 1$  to  $T$  do
4:   Forecast mixture:  $\rho_t^{\text{mix}} = \sum_{i=1}^N w_{t-1}^{(i)} \mathcal{N}(f(x_{t-1}^{(i)}), Q)$ .
5:   Forecast ensemble via TQMC:  $(\hat{x}_t^{(i)})_{i=1}^N = \text{TQMC}_N(\rho_t^{\text{mix}})$ .
6:   Kalman gain estimation (not required for QMC-BPF):
    • If  $h$  is nonlinear, compute  $K_t = \hat{C}_t^{xy} (\hat{C}_t^y)^{-1}$  via (5.9).
    • If  $h$  is linear, compute  $K_t = K_{p,t}$  via (5.12).
7:   Build proposals (not required for QMC-BPF):
    • For QMC-MMc and QMC-EnKFc, set  $q_t^{\text{mix}} = N^{-1} \sum_{i=1}^N q_{c,t}^{(i)}$  via (5.7).
    • For QMC-MMp and QMC-EnKFp, set  $q_t^{\text{mix}} = \sum_{i=1}^N w_{t-1}^{(i)} q_{p,t}^{(i)}$  via (5.8), cf. (7.1).
8:   Analysis ensemble via TQMC:
    • For QMC-BPF set  $\tilde{x}_t^{(i)} := \hat{x}_t^{(i)}$ .
    • Otherwise, set  $(\tilde{x}_t^{(i)})_{i=1}^N = \text{TQMC}_N(q_t^{\text{mix}})$ .
9:   Weights (self-normalized IS):
    • For QMC-BPF, set  $w_t^{(i)} \propto p(y_t | \tilde{x}_t^{(i)})$  and normalize.
    • For QMC-EnKFc and QMC-EnKFp, set  $w_t^{(i)} = \frac{1}{N}$ .
    • For QMC-MMc and QMC-MMp set  $w_t^{(i)} \propto \frac{p(y_t | \tilde{x}_t^{(i)}) \rho_t^{\text{mix}}(\tilde{x}_t^{(i)})}{q_t^{\text{mix}}(\tilde{x}_t^{(i)})}$  and normalize.
10:  No resampling: Set  $(x_t^{(i)})_{i=1}^N = (\tilde{x}_t^{(i)})_{i=1}^N$ .
11: end for

```

8. Numerical Experiments

We study three standard filtering problems (Evensen et al., 2022; Law et al., 2015) with dynamics and observation models of the form (5.1)–(5.2): the Lotka–Volterra model, the Lorenz–63 system and the Lorenz–96 system, introduced below. In all three models, the underlying dynamics is governed by an explicit ordinary differential equation (ODE) $z'(\tau) = \varphi(z(\tau))$ with closed-form right-hand side $\varphi: \mathbb{R}^d \rightarrow \mathbb{R}^d$, that is, denoting the flow operator of this ODE by Φ^τ , the dynamics model is given by $f = \Phi^{\Delta\tau}$ for a certain fixed time step $\Delta\tau > 0$. The initial distribution $p_0 = \mathcal{N}(m_0, \Sigma_0)$ of x_0 is chosen as a Gaussian with mean m_0 and covariance Σ_0 .

For each system, we consider two observation models,

- the (linear) identity observation function $h(x) = x$ with observation covariance $R = R_{\text{lin}} = (10\gamma)^{-2} I_d$,
- the nonlinear observation function $h(x) = \arctan(\frac{\gamma x}{20})$, applied componentwise, with observation covariance $R = R_{\text{nonlin}} = 10^{-4} I_d$.

Here, $\gamma > 0$ calibrates the operating scale of the models; accordingly we set $\Sigma_0 = Q = \gamma^{-2} I_d$ and $g(x) := \sin(4\gamma \sum_{j=1}^d x_j)$. The specific values of the parameters m_0 , $\Delta\tau$ and γ for each system are listed below and summarized in Table 8.1.

For each system and observation function, each time $t = 1, 2, 3$, each particle number⁵ $N \in \{2^2, \dots, 2^{10}\}$ and each of $M = 10$ independent random runs, every filtering method produces an ensemble estimate \hat{P}_t of the filtering distribution, which we compare to a reference approximation

⁵For the Lorenz–96 system with nonlinear h we are forced to start with $N = 2^6$ to ensure $N > d$, cf. Theorem 5.4.

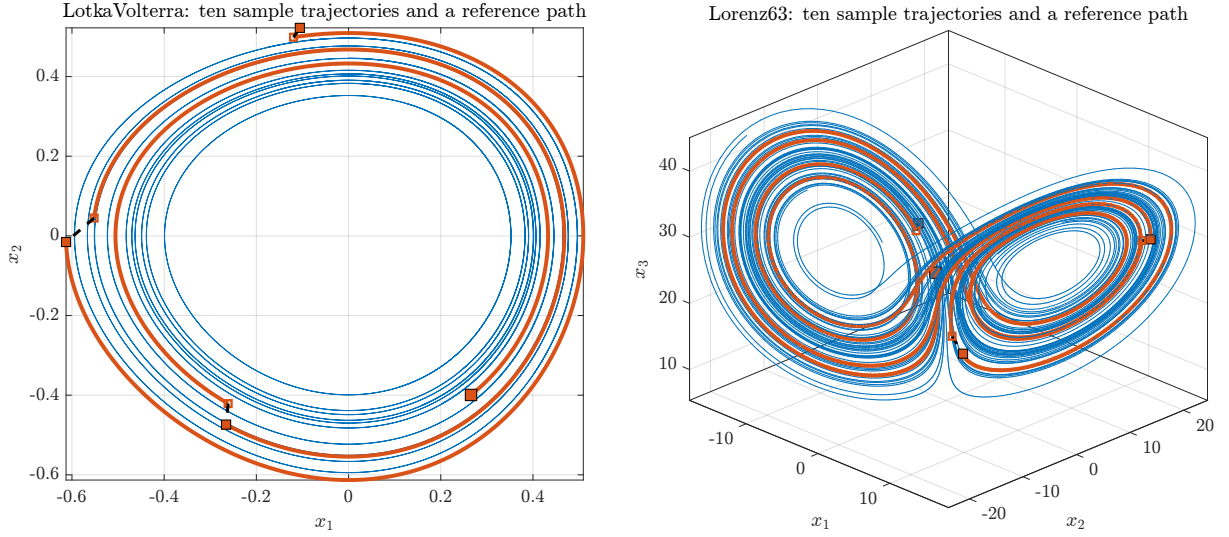


Figure 8.1: Sample ODE trajectories (blue) and underlying (true) perturbed dynamics (red) for the Lotka–Volterra model (left) and the Lorenz–63 model (right). The solid red lines correspond to the ODE transport $f = \Phi^{\Delta\tau}$ in (5.1) while the dotted black lines visualize the random perturbations η_t .

Table 8.1: Parameters used in the numerical experiments for each dynamical system.

System	m_0	$\Delta\tau$	γ
Lotka–Volterra	$\log(1.25, 0.66)^\top$	5	20
Lorenz–63	$(0, 0, 22)^\top$	2	1
Lorenz–96	0	0.5	4

$\hat{P}_{\text{ref},t}$ that is computed once per dataset using the QMC-MM_c estimator with $N_{\text{ref}} = 2^{13}$ particles ($N_{\text{ref}} = 2^{12}$ for the Lorenz–96 system):

$$\hat{P}_t = \sum_{i=1}^N w_t^{(i)} \delta_{\tilde{x}_t^{(i)}}, \quad \hat{P}_{\text{ref},t} = \sum_{i=1}^{N_{\text{ref}}} w_{\text{ref},t}^{(i)} \delta_{\tilde{x}_{\text{ref},t}^{(i)}}.$$

Note that the *pre-resampling* analysis ensembles are used, and that the same artificially generated observation data $(y_t)_{t=1}^T$ is used for all methods and each run. The comparison will be performed using two diagnostics, which are plotted against the particle numbers N in log-log scale in Figures 8.2 to 8.7: The mean absolute error (MAE)

$$\text{MAE}_t(N) = \left| \mathbb{E}_{\hat{P}_t}[g] - \mathbb{E}_{\hat{P}_{\text{ref},t}}[g] \right| = \left| \sum_{i=1}^N w_t^{(i)} g(\tilde{x}_t^{(i)}) - \sum_{i=1}^{N_{\text{ref}}} w_{\text{ref},t}^{(i)} g(\tilde{x}_{\text{ref},t}^{(i)}) \right|,$$

and the squared maximum mean discrepancy (MMD) between \hat{P}_t and $\hat{P}_{\text{ref},t}$ (Gretton et al., 2012)

$$\begin{aligned} \text{MMD}_{\kappa_t}^2(\hat{P}_t, \hat{P}_{\text{ref},t}) &= \sup_{\psi \in \mathcal{H}_{\kappa_t}} \left| \mathbb{E}_{\hat{P}_t}[\psi] - \mathbb{E}_{\hat{P}_{\text{ref},t}}[\psi] \right|^2 = \left\| \int \kappa_t(x, \cdot) \hat{P}_t(dx) - \int \kappa_t(x, \cdot) \hat{P}_{\text{ref},t}(dx) \right\|_{\mathcal{H}_{\kappa_t}}^2 \\ &= w_t^\top K_{XX} w_t + w_{\text{ref},t}^\top K_{RR} w_{\text{ref},t} - 2 w_t^\top K_{XR} w_{\text{ref},t}, \end{aligned}$$

where \mathcal{H}_{κ_t} is a reproducing kernel Hilbert space associated with a Gaussian RBF kernel κ_t , the bandwidth of which is set from the reference only (to make the kernel independent of the tested method and of N) using a median heuristic on pairwise distances,

$$\kappa_t(x, y) := \exp\left(-\frac{\|x-y\|^2}{2\ell_t^2}\right), \quad \ell_t^2 := \frac{\text{median}\{\|\tilde{x}_{\text{ref},t}^{(i)} - \tilde{x}_{\text{ref},t}^{(j)}\|^2 : 1 \leq i < j \leq N_{\text{ref}}\}}{\log N_{\text{ref}}},$$

and $[K_{XX}]_{ij} = \kappa_t(\tilde{x}_t^{(i)}, \tilde{x}_t^{(j)})$, $[K_{RR}]_{ij} = \kappa_t(\tilde{x}_{\text{ref},t}^{(i)}, \tilde{x}_{\text{ref},t}^{(j)})$ and $[K_{XR}]_{ij} = \kappa_t(\tilde{x}_t^{(i)}, \tilde{x}_{\text{ref},t}^{(j)})$.

Figures 8.2, 8.3, and 8.4 present our results for the three models, respectively, under the linear observation function $h(x) = Hx = x$. Similarly, Figures 8.5, 8.6, and 8.7 show the results under the nonlinear observation function $h(x) = \arctan(\frac{\gamma x}{20})$. Each figure has four rows, where the first two show the MAE and the last two the MMD², with the upper row comparing BPF and EnKF against the six EnKF reweighting schemes from Algorithm 2 across the three time steps $t = 1, 2, 3$ and the lower one showing how BPF, EnKF, MM^{str}_c, and MM^{str}_p improve when combined with TQMC points (indicated by markers), cf. Algorithm 4. Note that in the nonlinear case no schemes based on previous particles (those with the index p) are applicable (cf. Theorem 5.4), which is why the corresponding lines are absent from the plots.

For ease of reference, the interpretation of the numerical results is given directly in the caption of each figure. Overall, the mixture-weighted schemes improve accuracy and eliminate the EnKF error plateau caused by analysis-target mismatch, while the TQMC variants often yield additional gains by reducing sampling error. Before presenting the results, we briefly introduce the three models of interest:

Lotka–Volterra (Predator–Prey). As a prototypical example of biological interaction, we study the Lotka–Volterra equations, which capture the cyclic dynamics of predator and prey through a simple nonlinear feedback mechanism. We follow the nondimensionalized formulation introduced by (Murray, 2002, Section 3.1):

$$\dot{N} = N(1 - P), \quad \dot{P} = \alpha P(N - 1),$$

where N denotes the prey population size and P the predator population size and $\alpha > 0$ is a positive parameter. To ensure the positivity of the state variable under the addition of noise, we reformulate the system in logarithmic coordinates via $z = (u, v)^\top = (\log N, \log P)^\top$:

$$\dot{u} = 1 - e^v, \quad \dot{v} = \alpha(e^u - 1).$$

The parameters are chosen as follows: $\alpha = 1$ and $m_0 = (\log(1.25), \log(0.66))^\top$ (in accordance with the example of Murray 2002, Section 3.1), $\Delta\tau = 5$ and $\gamma = 20$.

Lorenz–63. The classical Lorenz 1963 system (Lorenz, 1963) is widely used as a low-dimensional benchmark for data assimilation methods due to its chaotic behavior. The system of three coupled nonlinear ordinary differential equations is given by

$$\begin{aligned} \dot{u} &= \sigma(v - u), \\ \dot{v} &= \rho u - v - uw, \\ \dot{w} &= uv - \beta w, \end{aligned}$$

where $z = (u, v, w)$ represents the system state and we use the standard parameter values $\sigma = 10$, $\rho = 28$, and $\beta = 8/3$, which lead to chaotic dynamics. The remaining parameters are chosen as follows: $\alpha = 1$ and $m_0 = (0, 0, 22)^\top$, $\Delta\tau = 2$ and $\gamma = 1$.

Lorenz-96. The Lorenz model from 1996 ([Lorenz, 1996](#)) serves as an example for a high-dimensional chaotic system. The model consists of d coupled scalar equations:

$$\dot{z}_j = (z_{j+1} - z_{j-2})z_{j-1} - z_j + F,$$

for $j = 1, \dots, d$. The parameters are chosen as follows: We set $d = 40$ and consider the forcing parameter $F = 8$. Further, $m_0 = 0$, $\Delta\tau = 0.5$ and $\gamma = 4$.

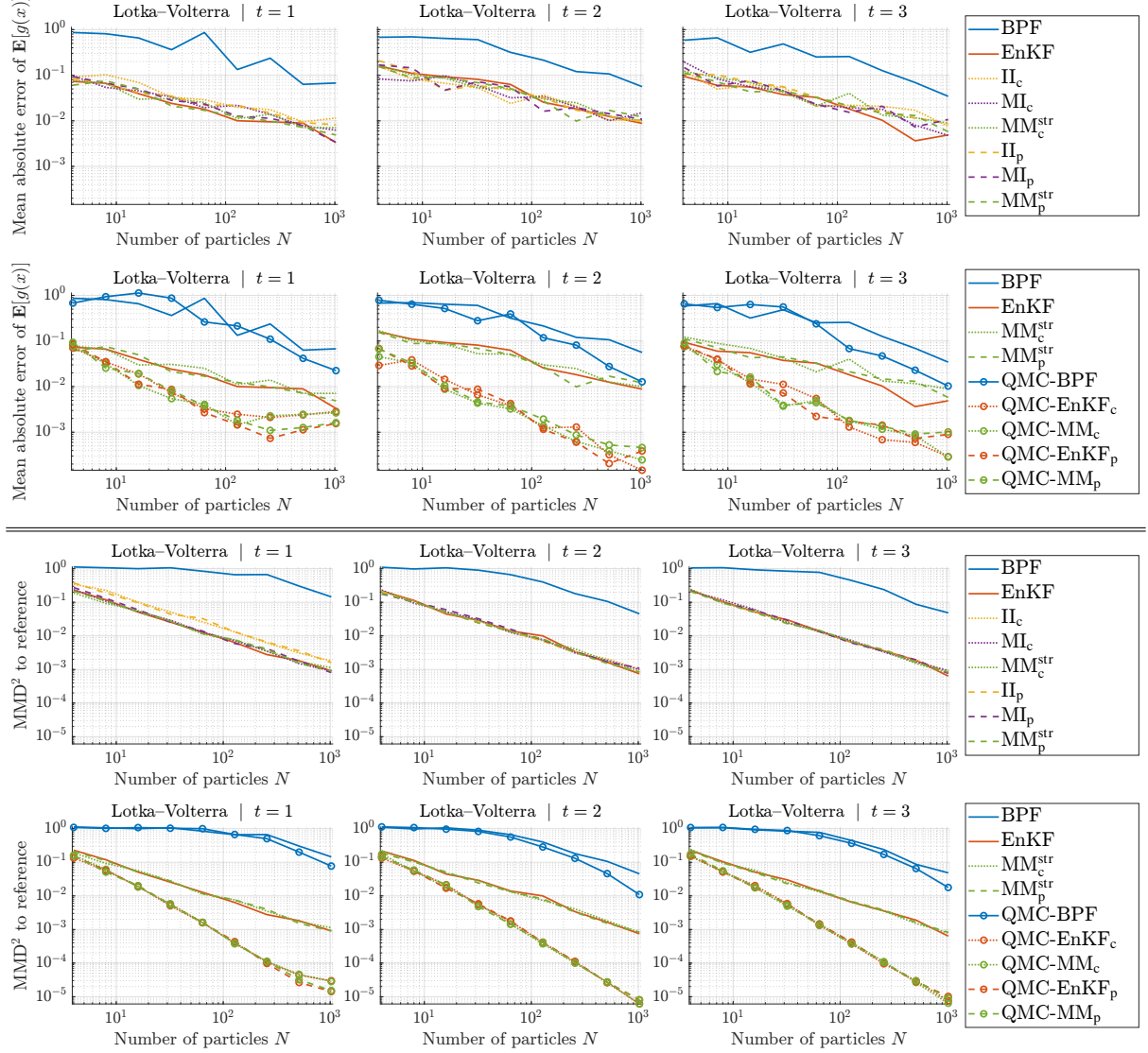


Figure 8.2: Results for the **Lotka–Volterra** model with **linear observation** function. The Lotka–Volterra flow is close to linear (nearly a rotation) over the ranges explored here. Therefore, under linear observations, the setting is almost linear–Gaussian and the EnKF almost consistent. Accordingly, all weighted EnKF variants exhibit very similar accuracy. By contrast, BPF displays substantially larger variance. Under *low observation noise* (sharp likelihood), only few prior particles land in the high–posterior–density region, which exacerbates weight degeneracy for BPF. Using TQMC point sets (indicated by markers) improves performance across methods by covering state space more evenly and thus enhancing the convergence rate.

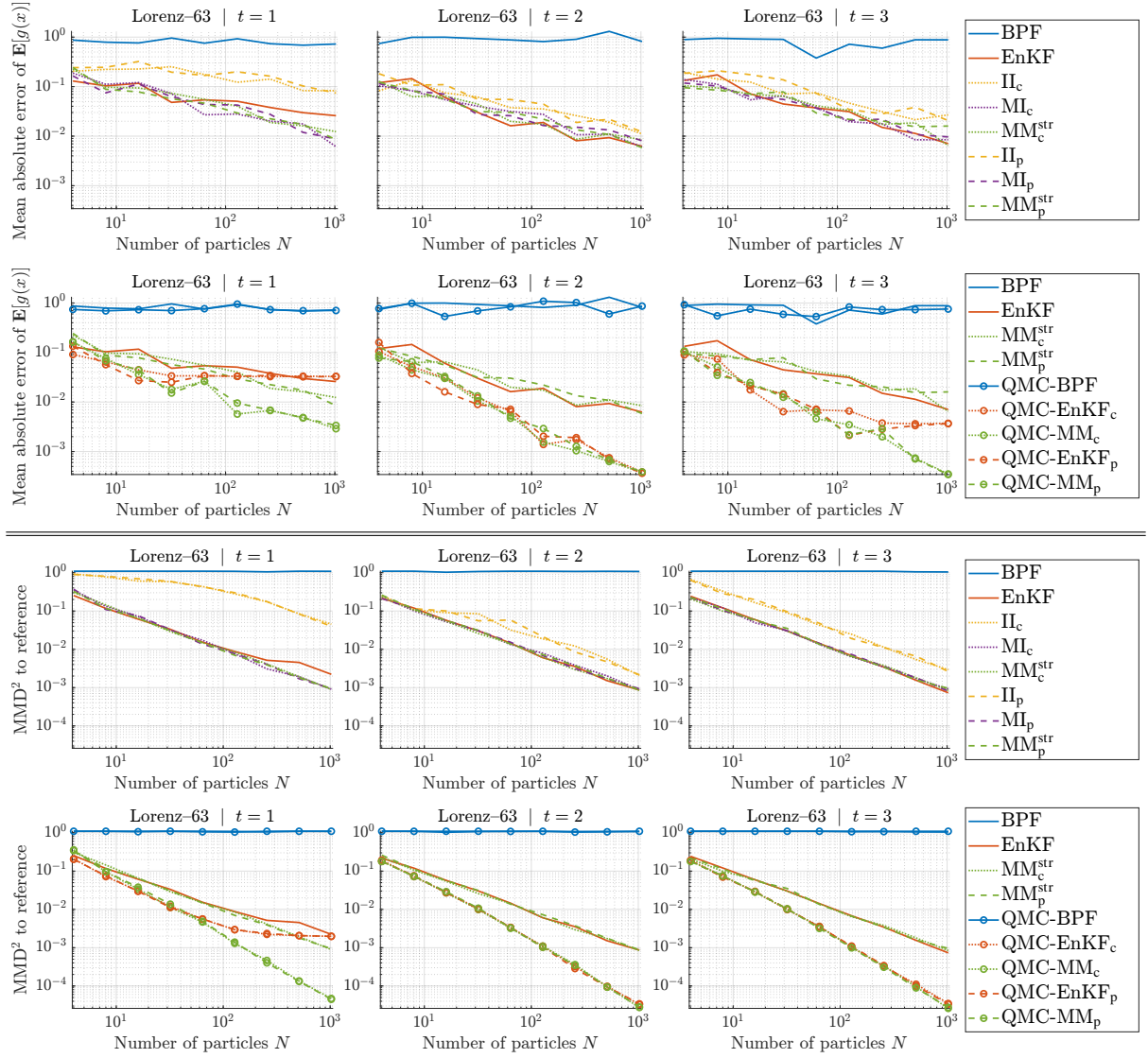


Figure 8.3: Results for the **Lorenz-63** model with **linear observation** function. At $t = 1$ the prior and posterior are strongly non-Gaussian, and the EnKF analysis-target mismatch introduces a bias that persists even as $N \rightarrow \infty$, yielding an early *error floor*. Among the weighted EnKF schemes, II_{\blacksquare} schemes perform worst throughout, consistent with the theoretically larger variance when individual proposals and individual targets place mass on different regions of state space. Averaging over components (MI_{\blacksquare} , MM^{str}) mitigates this effect and lowers variance. As assimilation proceeds ($t = 2, 3$), repeated conditioning pulls the forecast closer to Gaussianity, and the gap between EnKF and its weighted variants narrows. The penalty for using individual proposals against individual targets in II_{\blacksquare} also diminishes: the ensemble becomes more tightly clustered relative to the process-noise scale (set by Q), reducing the discrepancy between per-component targets and proposals. TQMC improves convergence for all six EnKF reweighting schemes but cannot remove the $t = 1$ saturation of the unweighted EnKF, which is bias dominated. For the BPF, severe weight degeneracy under low observation noise keeps the method far from the asymptotic regime over the N considered, so the rate improvement from TQMC would only become visible for much larger N (beyond the range shown).

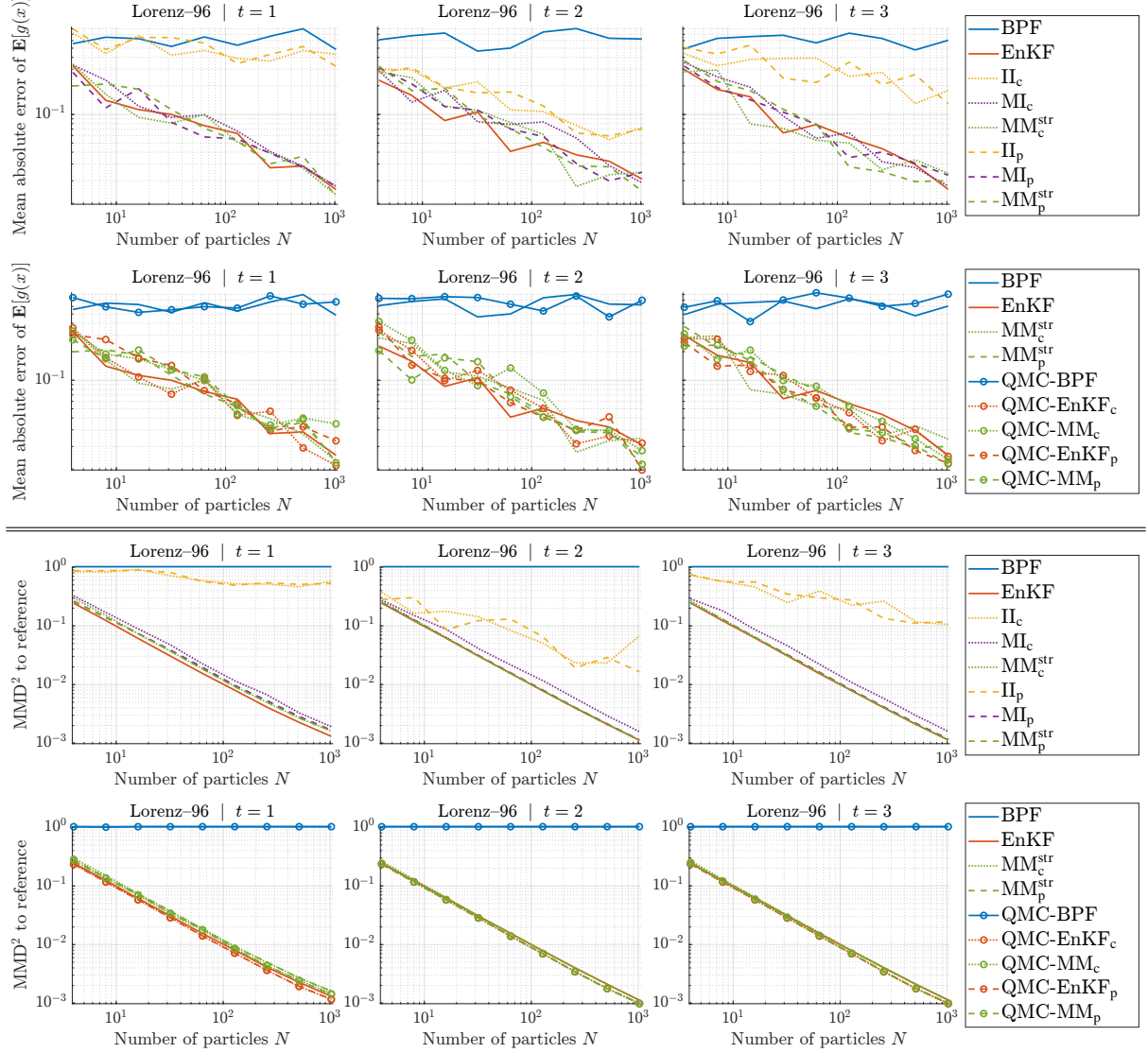


Figure 8.4: Results for the **Lorenz-96** model with **linear observation** function. As in the previous examples, the BPF fails to place a meaningful number of particles in the high-posterior-density region, leading to pronounced weight degeneracy. Among the EnKF-based methods, the II_{\square} schemes again perform worst. For this experiment, the remaining weighted EnKF schemes exhibit very similar errors to the vanilla EnKF over the range of ensemble sizes considered, so reweighting neither clearly improves nor degrades performance relative to the standard EnKF. However, in contrast to the vanilla EnKF, these weighted schemes come with consistency guarantees as $N \rightarrow \infty$ by [Theorem 6.1](#), so the results indicate that such guarantees can be obtained without sacrificing performance at the moderate ensemble sizes tested here. In this higher-dimensional setting ($d = 40$), using TQMC point sets does not lead to visible additional gains beyond the underlying schemes.

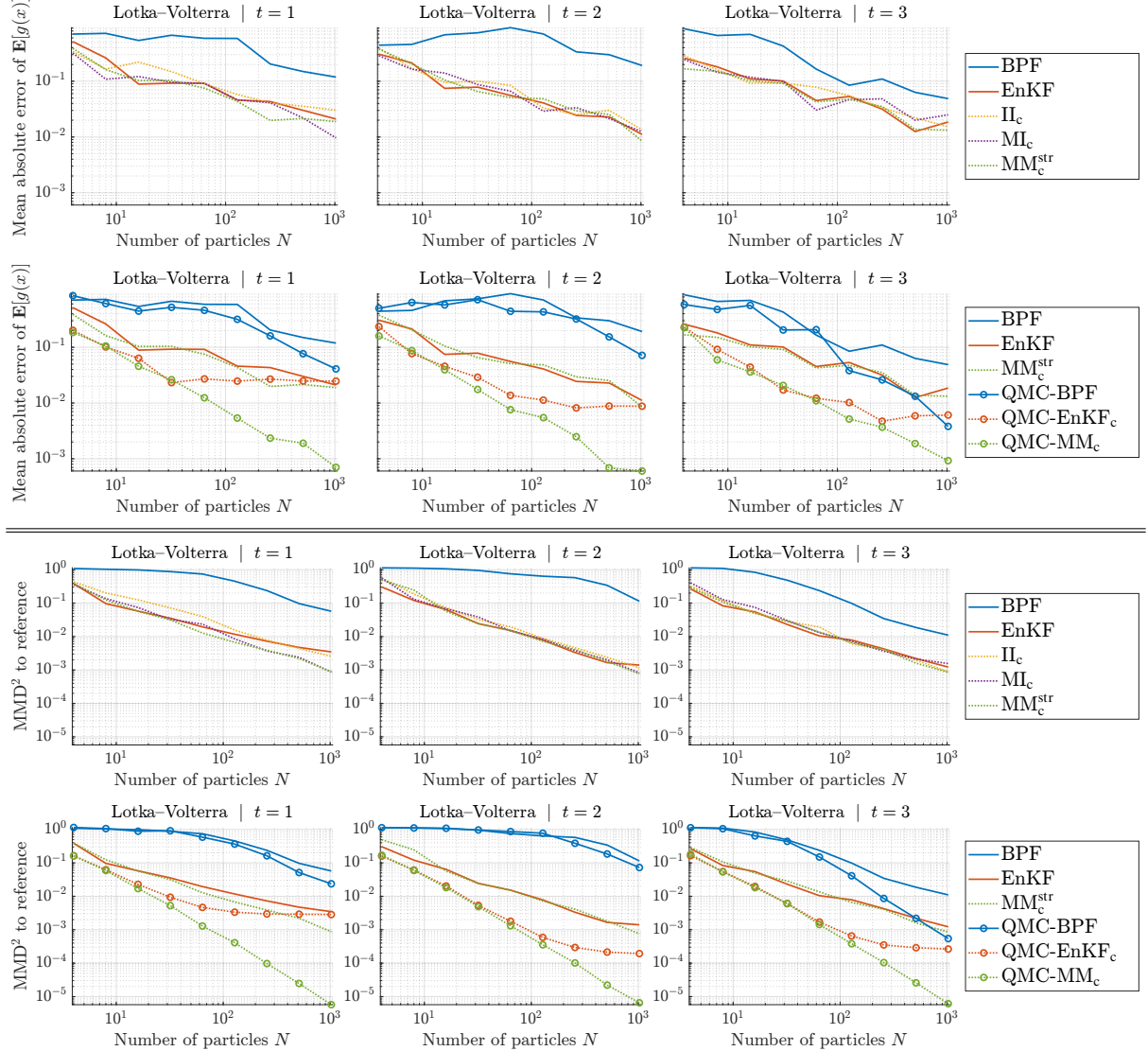


Figure 8.5: Results for the **Lotka–Volterra** model with **nonlinear observation** function. In this nonlinear and strongly non-Gaussian setting, the unweighted EnKF lacks consistency: its errors saturate for all times $t = 1, 2, 3$ and do not decrease beyond moderate ensemble sizes. For the weighted EnKF schemes, the improvement over the considered range of N is harder to see in the comparatively noisy MAE curves, but becomes more apparent in the MMD^2 plots, where the reweighted schemes continue to approach the reference distribution as N increases, while the unweighted EnKF reaches a floor. This effect is particularly visible for the TQMC-enhanced schemes, where the inconsistency of the vanilla EnKF prevents any analogous improvement in its TQMC variant.

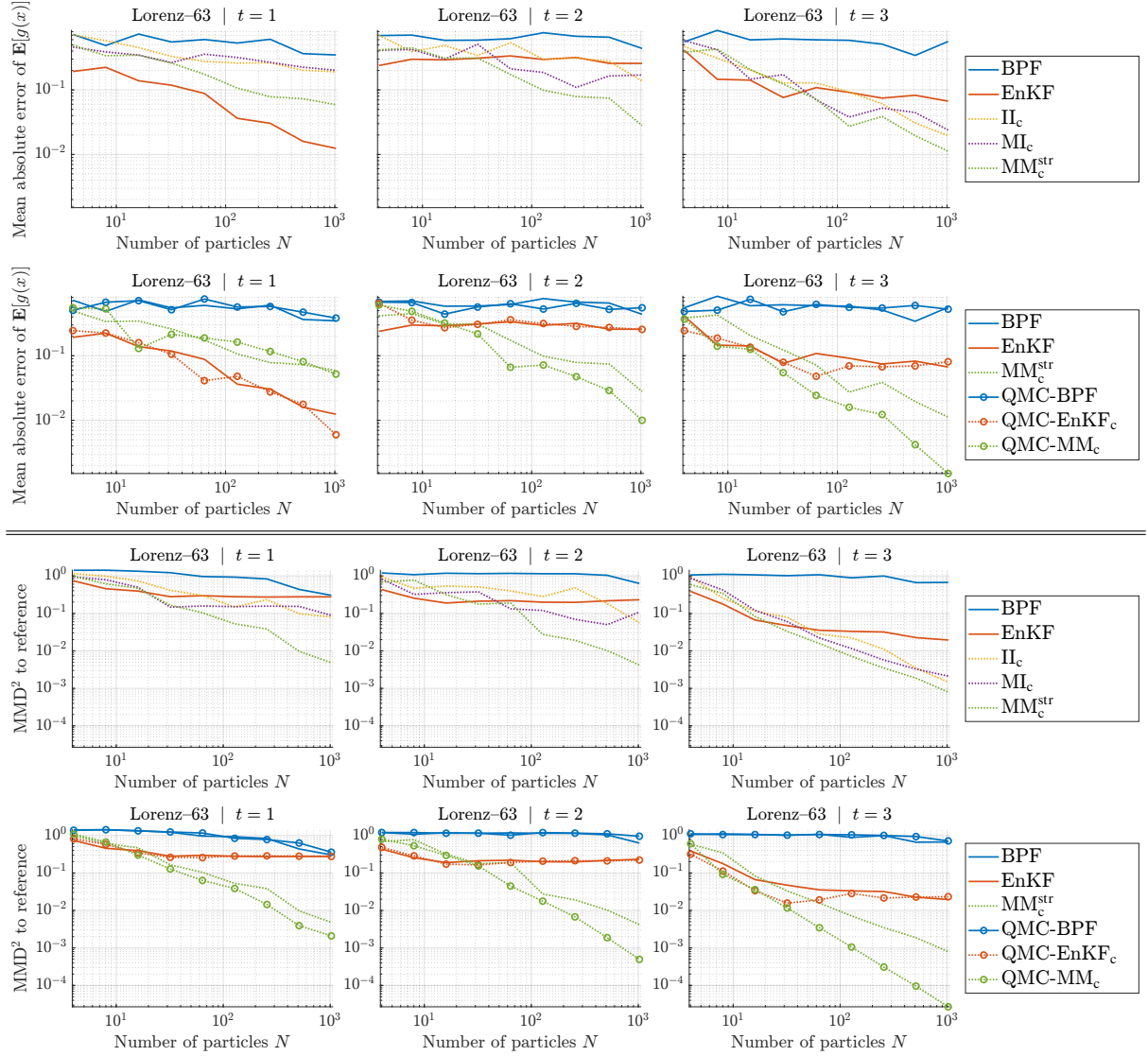


Figure 8.6: Results for the **Lorenz-63** model with **nonlinear observation** function. Compared to the linear observation case, the lack of consistency of the unweighted EnKF is even more pronounced: for all times $t = 1, 2, 3$ its error curves quickly hit a floor and show little improvement with increasing N , and the use of TQMC point sets does not alleviate this saturation. In contrast, the weighted EnKF schemes continue to improve with N and, for sufficiently large ensemble sizes, eventually outperform the vanilla EnKF, with the mixture-mixture scheme MM_c^{str} giving the best overall performance. The only exception is the MAE plot at $t = 1$, where the vanilla EnKF attains the smallest error for the particular test integrand g considered; however, it simultaneously performs very poorly in terms of MMD^2 , which measures the worst-case integration error over *all* integrands from the corresponding RKHS.

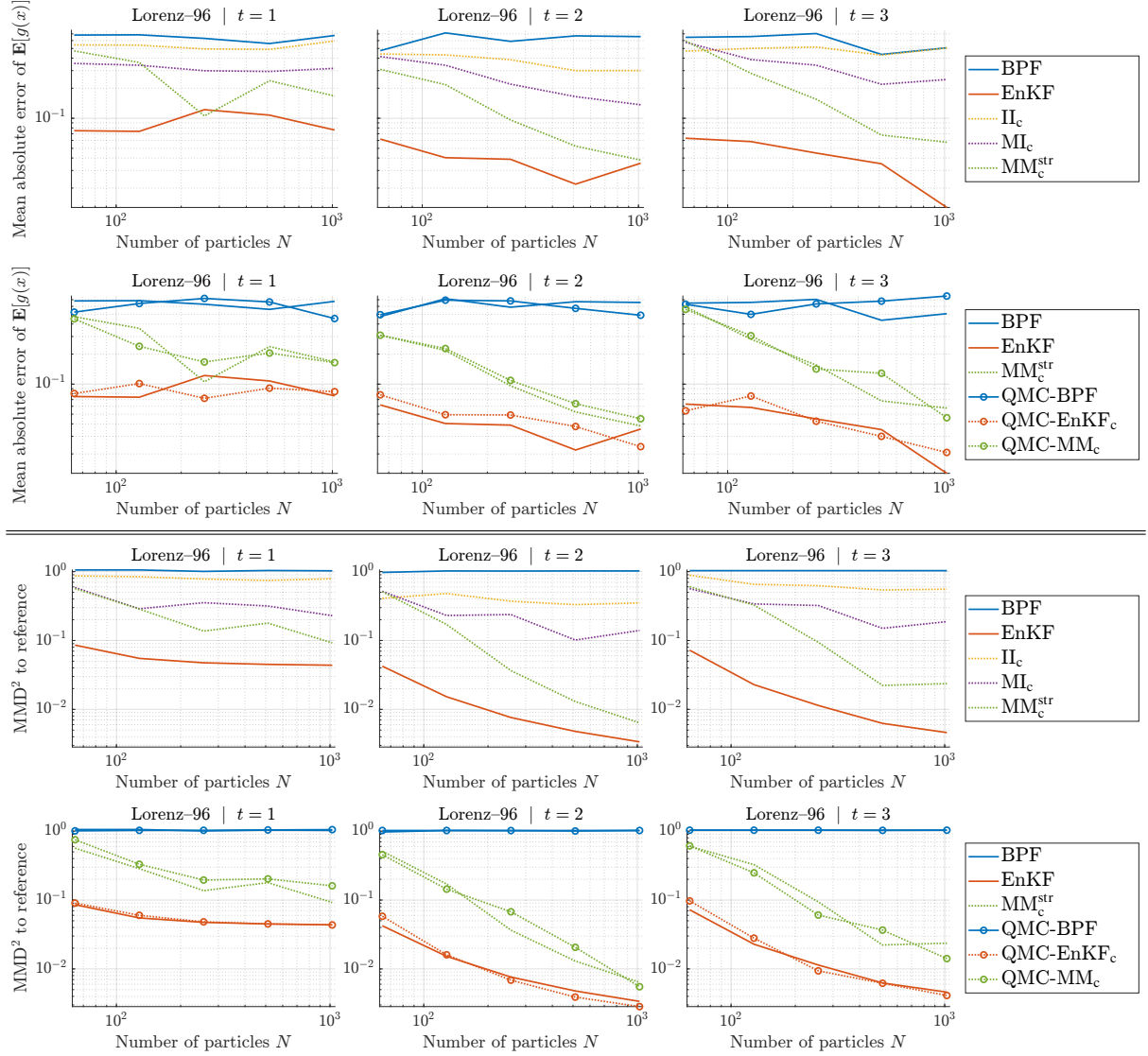


Figure 8.7: Results for the **Lorenz-96** model with **nonlinear observation** function. The mixture-based weighted EnKF schemes again outperform those with individual targets and proposals: across the range of ensemble sizes considered, MM_c^{str} performs best among the weighted schemes, followed by MI_c and then II_c . Throughout this experiment, the vanilla EnKF attains the smallest errors for the tested values of N , but the MMD^2 curves indicate a clear saturation of the EnKF as N increases, whereas the error of MM_c^{str} continues to decrease. In contrast to the vanilla EnKF, the weighted schemes (and in particular MM_c^{str}) come with consistency guarantees as $N \rightarrow \infty$ by [Theorem 6.1](#), so the observed behavior suggests that for sufficiently large ensemble sizes (beyond those shown here) MM_c^{str} would eventually cross and outperform the EnKF in terms of distributional accuracy. As in the linear observation case and consistent with the high dimension of the state space ($d = 40$), using TQMC point sets does not yield visible improvements over the corresponding Monte Carlo schemes.

9. Conclusion

We developed a unified importance-sampling framework for *mixture* targets and *mixture* proposals and used it to derive and analyze mixture-weighted variants of the EnKF. On the algorithmic side, we interpreted the stochastic EnKF analysis step as sampling from explicit Gaussian proposals and formalized both previous-ensemble and current-ensemble conditionals, enabling principled reweighting beyond the linear observation setting of the classical WEnKF. These constructions come with important applicability and stability caveats (in particular, linear-only availability of the previous-ensemble conditional, the WEnKF gain/proposal mismatch, and potential singularity issues), which we summarize in [Theorem 5.4](#). This led to six self-normalized IS-EnKF schemes, for which we proved consistency under a standard finite-variance condition on the importance weights ([Theorem 6.1](#)).

Our theoretical analysis identifies the (mean-one normalized) importance-weight variability, quantified by the squared coefficient of variation σ_t^2 , as the key quantity governing SNIS error bounds. Within our family of schemes we showed that using mixture targets together with mixture proposals minimizes σ_t ([Theorem 6.2](#)), thereby providing a rigorous justification for mixture-based reweighting. Moreover, for linear observations and bounded drift, we verified the key condition $\sigma_t < \infty$ required for consistency for two representative previous-ensemble schemes ([Theorem 6.3](#)), ensuring that the consistency theory applies in this setting. Our numerical experiments support these findings: mixture-based reweighting reduces weight degeneracy and improves estimation accuracy relative to per-component reweighting, and in regimes where the plain EnKF exhibits an N -independent error plateau due to analysis-target mismatch, the weighted schemes exhibit the expected decay with N .

To reduce sampling error in both prediction and analysis, we further proposed transported quasi-Monte Carlo (TQMC) for Gaussian mixtures ([Section 7](#)), yielding TQMC-enhanced variants of BPF, EnKF, and their mixture-weighted counterparts with substantial gains in low-to-moderate dimensions for consistent methods and competitive performance in higher-dimensional tests. Naturally, TQMC addresses sampling variance only and cannot resolve the EnKF analysis-target mismatch, so any associated error saturation persists — providing an additional motivation to employ weighted EnKF variants.

Several directions remain for future work. First, it would be valuable to extend the finite-variance theory beyond the presently covered cases, in particular to broader classes of current-ensemble schemes, nonlinear observation models h and unbounded drifts f . Second, combining mixture-weighted reweighting with standard EnKF stabilizations such as localization and inflation is an important step towards large-scale applications: since the reweighting step targets the correct filtering distribution asymptotically, it does not introduce the systematic bias that can accompany localization or inflation, and instead offers a principled route to mitigate analysis-target mismatch while retaining the practical benefits of these stabilizations. Third, for nonlinear observation maps h , a key open problem is how to control the range-related singularities highlighted in [Theorem 5.4](#) and to design robust proposals and reweighting strategies that avoid weight blow-up. Finally, it remains to better understand how (transported) QMC should be deployed in data assimilation, in particular in higher dimensions where low-discrepancy structure, transport quality, and the sequential nature of the problem interact in subtle ways.

A. Counterexamples to additional variance inequalities between the estimators II , MI , IM , MM and MM^{str}

Theorem 4.1 shows that, for any $g \in L^2(p_{\text{mix}})$,

$$\mathbb{V}[\text{MM}^{\text{str}}(g)] \leq \mathbb{V}[\text{MM}(g)] \leq \min(\mathbb{V}[\text{IM}(g)], \mathbb{V}[\text{MI}(g)]).$$

In particular, the “mixture-mixture” estimators MM and MM^{str} are never worse (in variance) than either IM or MI . The goal of this appendix is to show that *no further* general variance inequalities between the five estimators II , MI , IM , MM and MM^{str} from Section 4 hold: for every pair of estimators that is not ordered by the display above, both directions of the inequality can occur for suitable choices of (p_i, q_i, g) .

For simplicity, throughout this section, we work on a two-point state space $X = \{0, 1\}$ with $N = 2$ components, noting that these discrete examples can be embedded without difficulty into the setting of Theorem 4.1. We represent probability mass functions on X by two-dimensional vectors and write, for example, $p = (\alpha, \beta)$ to mean $p(0) = \alpha$ and $p(1) = \beta$.

Example A.1 ($\mathbb{V}[\text{II}(1)] > \mathbb{V}[\text{IM}(1)] > \mathbb{V}[\text{MI}(1)]$). We construct the example so that $p_{\text{mix}} = q_{\text{mix}}$ for $g \equiv 1$, which makes the mixture-mixture estimators MM and MM^{str} *deterministic*, while the “individual” estimators II , IM and MI still have strictly positive (but different) variances. Let $g \equiv 1$ and choose

$$p_1 = \left(\frac{1}{10}, \frac{9}{10}\right), \quad p_2 = \left(\frac{2}{5}, \frac{3}{5}\right), \quad q_1 = \left(\frac{3}{10}, \frac{7}{10}\right), \quad q_2 = \left(\frac{1}{5}, \frac{4}{5}\right).$$

Then

$$p_{\text{mix}} = \frac{1}{2}(p_1 + p_2) = \left(\frac{1}{4}, \frac{3}{4}\right), \quad q_{\text{mix}} = \frac{1}{2}(q_1 + q_2) = \left(\frac{1}{4}, \frac{3}{4}\right),$$

so $p_{\text{mix}} = q_{\text{mix}}$ and $p_{\text{mix}} \ll q_i$ holds for $i = 1, 2$. All five estimators target $I = \mathbb{E}_{p_{\text{mix}}}[g] = 1$. Since $p_{\text{mix}} = q_{\text{mix}}$ and $g \equiv 1$, each summand in $\text{MM}(g)$ and $\text{MM}^{\text{str}}(g)$ is identically g and therefore $\mathbb{V}[\text{MM}(g)] = \mathbb{V}[\text{MM}^{\text{str}}(g)] = 0$. In contrast, the pairs (p_i, q_i) are not aligned for $i = 1, 2$, so the ratios p_i/q_i , p_i/q_{mix} and p_{mix}/q_i are all non-constant on X , and the estimators $\text{II}(g)$, $\text{IM}(g)$ and $\text{MI}(g)$ remain random. A direct calculation of the variances gives

$$\mathbb{V}[\text{II}(g)] = \frac{37}{336} > \mathbb{V}[\text{IM}(g)] = \frac{3}{50} > \mathbb{V}[\text{MI}(g)] = \frac{37}{5376} > \mathbb{V}[\text{MM}(g)] = \mathbb{V}[\text{MM}^{\text{str}}(g)] = 0.$$

Example A.2 ($\mathbb{V}[\text{MI}(g)] > \mathbb{V}[\text{IM}(g)] > \mathbb{V}[\text{MM}(g)] > \mathbb{V}[\text{MM}^{\text{str}}(g)] > \mathbb{V}[\text{II}(g)]$). We now construct an example in which II has *zero* variance, while the other four estimators have strictly positive variance, and at the same time $\mathbb{V}[\text{MI}(g)] > \mathbb{V}[\text{IM}(g)]$. Let

$$q_1 = \left(\frac{2}{3}, \frac{1}{3}\right), \quad q_2 = \left(\frac{1}{3}, \frac{2}{3}\right), \quad g = (1, 2).$$

We now choose p_1, p_2 so that, for each $i = 1, 2$, the quantity $(p_i/q_i)g$ is constant on X , that is

$$\frac{p_i(0)}{q_i(0)}g(0) = \frac{p_i(1)}{q_i(1)}g(1).$$

These conditions yield

$$\frac{p_1(0)}{p_1(1)} = \frac{q_1(0)g(1)}{q_1(1)g(0)} = \frac{\frac{2}{3} \cdot 2}{\frac{1}{3} \cdot 1} = 4, \quad \frac{p_2(0)}{p_2(1)} = \frac{q_2(0)g(1)}{q_2(1)g(0)} = \frac{\frac{1}{3} \cdot 2}{\frac{2}{3} \cdot 1} = 1,$$

and thereby $p_1 = (\frac{4}{5}, \frac{1}{5})$ and $p_2 = (\frac{1}{2}, \frac{1}{2})$. Then $q_{\text{mix}} = \frac{1}{2}(q_1 + q_2) = (\frac{1}{2}, \frac{1}{2})$ and $p_{\text{mix}} = \frac{1}{2}(p_1 + p_2) = (\frac{13}{20}, \frac{7}{20})$, so $p_{\text{mix}} \ll q_i$ holds for $i = 1, 2$. By construction, each summand in

$$\text{II}(g) = \frac{1}{2} \left(\frac{p_1(X_1)}{q_1(X_1)} g(X_1) + \frac{p_2(X_2)}{q_2(X_2)} g(X_2) \right)$$

is constant, implying $\mathbb{V}[\text{II}(g)] = 0$. Further, a direct computation gives

$$\mathbb{V}[\text{MI}(g)] = \frac{369}{3200} > \mathbb{V}[\text{IM}(g)] = \frac{41}{400} > \mathbb{V}[\text{MM}(g)] = \frac{1}{800} > \mathbb{V}[\text{MM}^{\text{str}}(g)] = \frac{1}{900} > \mathbb{V}[\text{II}(g)] = 0.$$

Hence, for every pair $(A, B) \in \{\text{II}, \text{MI}, \text{IM}, \text{MM}, \text{MM}^{\text{str}}\}$ of distinct estimators that is not already ordered by Theorem 4.1, we see that both inequalities $\mathbb{V}[A(g)] < \mathbb{V}[B(g)]$ and $\mathbb{V}[A(g)] > \mathbb{V}[B(g)]$ can arise for suitable choices of (p_i, q_i, g) . No additional general variance inequalities between $\text{II}, \text{MI}, \text{IM}, \text{MM}$ and MM^{str} therefore hold beyond those stated in Theorem 4.1.

B. Auxiliary Results for the Proof of Theorem 6.1

We now provide details for the proof of Theorem 6.1. In particular, we derive the bounds required to control the three contributing error terms: the approximation error for the filtering distribution, the self-normalized importance sampling (SNIS) error, and the resampling error.

Lemma B.1 (approximation error for the filtering distribution). *Under the assumptions of Theorem 6.1 and using the notation therein,*

$$d\left(p_t^{\text{post}}, \frac{p_t^{\text{mix}}}{Z_t^{\text{mix}}}\right) \leq \frac{2d_{t-1}}{Z_t^{\text{post}}}, \quad t = 1, \dots, T. \quad (\text{B.1})$$

Proof. Let $g \in \mathcal{C}_b(\mathbb{R}^d)$ with $\|g\|_{\infty} \leq 1$. Since $0 \leq \ell_t \leq 1$, we also have $\ell_t, g\ell_t \in \mathcal{C}_b(\mathbb{R}^d)$ with $\|g\ell_t\|_{\infty} \leq \|\ell_t\|_{\infty} \leq 1$, and thereby

$$\begin{aligned} E_1(g) &:= \mathbb{E} \left[\left(\int g \ell_t \pi_t^{\text{prior}} - \int g \ell_t \pi_t^{\text{mix}} \right)^2 \right] \leq d(\pi_t^{\text{prior}}, \pi_t^{\text{mix}})^2 \\ E_2(g) &:= \mathbb{E} \left[\left(\int g \frac{p_t^{\text{mix}}}{Z_t^{\text{mix}}} \right)^2 (Z_t^{\text{post}} - Z_t^{\text{mix}})^2 \right] \leq \mathbb{E}[(Z_t^{\text{post}} - Z_t^{\text{mix}})^2] \\ &= \mathbb{E} \left[\left(\int \ell_t \pi_t^{\text{prior}} - \int \ell_t \pi_t^{\text{mix}} \right)^2 \right] \leq d(\pi_t^{\text{prior}}, \pi_t^{\text{mix}})^2. \end{aligned} \quad (\text{B.2})$$

By Bayes' theorem,

$$\begin{aligned} p_t^{\text{post}} - \frac{p_t^{\text{mix}}}{Z_t^{\text{mix}}} &= \frac{\ell_t \pi_t^{\text{prior}}}{Z_t^{\text{post}}} - \frac{\ell_t \pi_t^{\text{mix}}}{Z_t^{\text{mix}}} \\ &= \frac{\ell_t \pi_t^{\text{prior}}}{Z_t^{\text{post}}} - \frac{\ell_t \pi_t^{\text{mix}}}{Z_t^{\text{post}}} + \frac{\ell_t \pi_t^{\text{mix}}}{Z_t^{\text{post}}} - \frac{\ell_t \pi_t^{\text{mix}}}{Z_t^{\text{mix}}} \\ &= \frac{\ell_t \pi_t^{\text{prior}} - \ell_t \pi_t^{\text{mix}}}{Z_t^{\text{post}}} + \frac{\ell_t \pi_t^{\text{mix}}}{Z_t^{\text{mix}}} \frac{Z_t^{\text{mix}} - Z_t^{\text{post}}}{Z_t^{\text{post}}}, \end{aligned}$$

which, together with (B.2) and the triangle inequality, implies

$$\begin{aligned}
d\left(p_t^{\text{post}}, \frac{p_t^{\text{mix}}}{Z_t^{\text{mix}}}\right) &= \sup_{\|g\|_\infty \leq 1} \mathbb{E} \left[\left(\int g \left(p_t^{\text{post}} - \frac{p_t^{\text{mix}}}{Z_t^{\text{mix}}} \right) \right)^2 \right]^{1/2} \\
&\leq \sup_{\|g\|_\infty \leq 1} \frac{\sqrt{E_1(g)} + \sqrt{E_2(g)}}{Z_t^{\text{post}}} \\
&\leq \frac{2}{Z_t^{\text{post}}} d(\pi_t^{\text{prior}}, \pi_t^{\text{mix}}) \\
&\leq \frac{2}{Z_t^{\text{post}}} d\left(p_{t-1}^{\text{post}}, \frac{1}{N} \sum_{i=1}^N \delta_{x_{t-1}^{(i)}}\right),
\end{aligned}$$

where the last inequality follows from (Sanz-Alonso et al., 2023, Lemma 11.2). \blacksquare

Lemma B.2 (SNIS error). *Under the assumptions of Theorem 6.1 and using the notation therein,*

$$d\left(\frac{p_t^{\text{mix}}}{Z_t^{\text{mix}}}, \sum_{i=1}^N w_t^{(i)} \delta_{\tilde{x}_t^{(i)}}\right) \leq \frac{2\sigma_t + 1}{\sqrt{N}}, \quad t = 1, \dots, T.$$

Proof. We introduce the σ -algebra \mathcal{F}_t generated by “the history we condition upon”:

$$\mathcal{F}_t = \sigma((x_{t-1}^{(j)})_{j=1}^N, (\hat{x}_t^{(j)})_{j=1}^N).$$

Let $g \in \mathcal{C}_b(\mathbb{R}^d)$ with $\|g\|_\infty \leq 1$. Since $\frac{1}{N} \sum_{i=1}^N \frac{\check{p}_t^{(i)}}{\check{q}_t^{(i)}} q_t^{(i)} = p_t^{\text{mix}}$ for each sampling scheme,

$$\mathbb{E} \left[\frac{1}{N} \sum_{i=1}^N g(\tilde{x}_t^{(i)}) \frac{v_t^{(i)}}{Z_t^{\text{mix}}} \middle| \mathcal{F}_t \right] = \mathbb{E} \left[\frac{1}{N} \sum_{i=1}^N \frac{g \check{p}_t^{(i)}}{Z_t^{\text{mix}} \check{q}_t^{(i)}} (\tilde{x}_t^{(i)}) \middle| \mathcal{F}_t \right] = \frac{1}{N} \sum_{i=1}^N \int \frac{g \check{p}_t^{(i)}}{Z_t^{\text{mix}} \check{q}_t^{(i)}} q_t^{(i)} = \int \frac{g p_t^{\text{mix}}}{Z_t^{\text{mix}}}, \quad (\text{B.3})$$

$$\mathbb{E} \left[\frac{v_t^{(1)}}{Z_t^{\text{mix}}} \right] = \frac{1}{N} \sum_{i=1}^N \mathbb{E} \left[\frac{v_t^{(i)}}{Z_t^{\text{mix}}} \right] = \mathbb{E} \left[\mathbb{E} \left[\frac{1}{N} \sum_{i=1}^N \frac{v_t^{(i)}}{Z_t^{\text{mix}}} \middle| \mathcal{F}_t \right] \right] \stackrel{(*)}{=} \mathbb{E} \left[\int \frac{p_t^{\text{mix}}}{Z_t^{\text{mix}}} \right] = 1, \quad (\text{B.4})$$

where (*) is an application of (B.3) for $g \equiv 1$. In (B.4) we used that, by the symmetry of

$$q_t^{(i)} = \mathfrak{q} \left(x_{t-1}^{(i)}, \hat{x}_t^{(i)}, \frac{1}{N} \sum_{j=1}^N \delta_{x_{t-1}^{(j)}}, \frac{1}{N} \sum_{j=1}^N \delta_{\hat{x}_t^{(j)}}, y_t \right)$$

with respect to the particles $(x_{t-1}^{(j)})_{j=1}^N$ in the third and $(\hat{x}_t^{(j)})_{j=1}^N$ in fourth argument, cf. (6.6), each family of corresponding random variables is exchangeable across the indices $i = 1, \dots, N$, in particular, the weights $v_t^{(i)}$ have the same distribution. Thereby, using the laws of total

expectation and total variance as well as $\|g\|_\infty \leq 1$,

$$\begin{aligned}
 E_1(g) &:= \mathbb{E} \left[\left(\int g \frac{p_t^{\text{mix}}}{Z_t^{\text{mix}}} - \frac{1}{N} \sum_{i=1}^N g(\tilde{x}_t^{(i)}) \frac{v_t^{(i)}}{Z_t^{\text{mix}}} \right)^2 \right] \\
 &= \mathbb{E} \left[\mathbb{V} \left[\frac{1}{N} \sum_{i=1}^N g(\tilde{x}_t^{(i)}) \frac{v_t^{(i)}}{Z_t^{\text{mix}}} \mid \mathcal{F}_t \right] \right] \\
 &= \frac{1}{N} \mathbb{E} \left[\mathbb{V} \left[g(\tilde{x}_t^{(1)}) \frac{v_t^{(1)}}{Z_t^{\text{mix}}} \mid \mathcal{F}_t \right] \right] \\
 &\leq \frac{1}{N} \mathbb{E} \left[\left(g(\tilde{x}_t^{(1)}) \frac{v_t^{(1)}}{Z_t^{\text{mix}}} \right)^2 \right] \\
 &\leq \frac{1}{N} \mathbb{E} \left[\left(\frac{v_t^{(1)}}{Z_t^{\text{mix}}} \right)^2 \right] \\
 &= \frac{1}{N} \left(\mathbb{V} \left[\frac{v_t^{(1)}}{Z_t^{\text{mix}}} \right] + \mathbb{E} \left[\frac{v_t^{(1)}}{Z_t^{\text{mix}}} \right]^2 \right) \\
 &= \frac{\sigma_t^2 + 1}{N}.
 \end{aligned}$$

Since $w_t^{(i)} = v_t^{(i)} / \sum_j v_t^{(j)}$ and $\|g\|_\infty \leq 1$, (B.4) implies

$$\begin{aligned}
 E_2(g) &:= \mathbb{E} \left[\left(\frac{1}{N} \sum_{i=1}^N g(\tilde{x}_t^{(i)}) \frac{v_t^{(i)}}{Z_t^{\text{mix}}} - \sum_{i=1}^N g(\tilde{x}_t^{(i)}) w_t^{(i)} \right)^2 \right] \\
 &= \mathbb{E} \left[\left(\sum_{i=1}^N g(\tilde{x}_t^{(i)}) w_t^{(i)} \right)^2 \left(\frac{1}{N} \sum_{j=1}^N \frac{v_t^{(j)}}{Z_t^{\text{mix}}} - 1 \right)^2 \right] \\
 &\leq \mathbb{E} \left[\left(\frac{1}{N} \sum_{j=1}^N \frac{v_t^{(j)}}{Z_t^{\text{mix}}} - 1 \right)^2 \right] \\
 &= \mathbb{V} \left[\frac{1}{N} \sum_{j=1}^N \frac{v_t^{(j)}}{Z_t^{\text{mix}}} \right] \\
 &= \frac{\sigma_t^2}{N}.
 \end{aligned}$$

Using the triangle inequality, it follows that

$$\begin{aligned}
 d \left(\frac{p_t^{\text{mix}}}{Z_t^{\text{mix}}}, \sum_{i=1}^N w_t^{(i)} \delta_{\tilde{x}_t^{(i)}} \right) &= \sup_{\|g\|_\infty \leq 1} \mathbb{E} \left[\left(\int g \frac{p_t^{\text{mix}}}{Z_t^{\text{mix}}} - \sum_{i=1}^N g(\tilde{x}_t^{(i)}) w_t^{(i)} \right)^2 \right]^{1/2} \\
 &\leq \sup_{\|g\|_\infty \leq 1} (\sqrt{E_1(g)} + \sqrt{E_2(g)}) \\
 &\leq \frac{\sigma_t + 1}{\sqrt{N}} + \frac{\sigma_t}{\sqrt{N}}.
 \end{aligned}$$

■

Lemma B.3 (resampling error; adaptation of [Chopin and Papaspiliopoulos 2020](#), Lemma 11.1).
Under the assumptions of [Theorem 6.1](#) and using the notation therein,

$$d \left(\sum_{i=1}^N w_t^{(i)} \delta_{\tilde{x}_t^{(i)}}, \frac{1}{N} \sum_{i=1}^N \delta_{x_t^{(i)}} \right) \leq \frac{1}{\sqrt{N}}, \quad t = 1, \dots, T.$$

Proof. Due to (5.5), $\mathbb{E}\left[\frac{1}{N} \sum_{i=1}^N g(x_t^{(i)}) \mid \{\tilde{x}_t^{(i)}\}\right] = \sum_{i=1}^N w_t^{(i)} g(\tilde{x}_t^{(i)})$. Therefore,

$$d\left(\sum_{i=1}^N w_t^{(i)} \delta_{\tilde{x}_t^{(i)}}, \frac{1}{N} \sum_{i=1}^N \delta_{x_t^{(i)}}\right)^2 = \sup_{\|g\|_\infty \leq 1} \mathbb{E}\left[\mathbb{V}\left[\frac{1}{N} \sum_{i=1}^N g(x_t^{(i)}) \mid \{\tilde{x}_t^{(i)}\}\right]\right] \leq \frac{1}{N},$$

since the supremum is taken over functions g which satisfy $g(x_t^{(i)})^2 \leq 1$. \blacksquare

C. Auxiliary Results for the Proof of Theorem 6.3

We will now show the details for each step in the proof of Theorem 6.3, using the assumptions and notation therein. For this purpose, we begin by introducing certain Kalman and EnKF matrices and establishing their relations, which we will use throughout this section:⁶

$$\begin{aligned} Q &\in \mathbf{S}_{++}^d & Q_t &:= \hat{C}_t^{x,\mathbf{p}} = \mathbb{C}\text{ov}^{\text{emp}}\left[(f(x_{t-1}^{(i)}))_{i=1}^N\right] + Q \in \mathbf{S}_{++}^d, \\ S &:= HQH^\top + R \in \mathbf{S}_{++}^m, & S_t &:= HQ_t H^\top + R \in \mathbf{S}_{++}^m, \\ K &:= QH^\top S^{-1} \in \mathbb{R}^{d \times m}, & K_t &:= K_t^{\mathbf{p}} = Q_t H^\top S_t^{-1} \in \mathbb{R}^{d \times m}, \\ \Sigma &:= (I_d - KH)Q(I_d - KH)^\top + KRK^\top, & \Sigma_t &:= \Sigma_{\mathbf{p},t} = (I_d - K_t H)Q(I_d - K_t H)^\top + K_t R K_t^\top, \end{aligned}$$

cf. (5.12) for the definition of $\hat{C}_t^{x,\mathbf{p}}$ and $K_t^{\mathbf{p}}$ and (5.8) for the definition of $\Sigma_{\mathbf{p},t}$. We also denote

$$\Delta_Q := Q_t - Q, \quad \Delta_K := K_t - K, \quad \Delta_\Sigma := \Sigma_t - \Sigma.$$

Lemma C.1 (EnKF matrix identities). *The above-defined matrices satisfy:*

- (i) $\Sigma = Q - KHQ$, in line with its definition in Theorem 6.3;
- (ii) $\Sigma H^\top = KR$;
- (iii) $\det \Sigma \det S = \det Q \det R$, in particular, $\Sigma \in \mathbf{S}_{++}^d$ is strictly positive definite;
- (iv) $\Delta_K = (I_d - K_t H) \Delta_Q H^\top S^{-1}$;
- (v) $\Delta_\Sigma = \Delta_K S \Delta_K^\top$ and $\text{ran}(\Delta_\Sigma) = \text{ran}(\Delta_K)$, in particular, $\Delta_\Sigma \in \mathbf{S}_+^d$ and $\Sigma_t \in \mathbf{S}_{++}^d$.

Proof. (i) follows from resolving the parentheses in the definition of Σ :

$$\Sigma = Q - KHQ - QH^\top K^\top + K(HQH^\top + R)K^\top = Q - KHQ - QH^\top K^\top + QH^\top S^{-1} SK^\top.$$

By (i), $\Sigma H^\top = QH^\top - KHQH^\top = K(S - HQH^\top) = KR$, proving (ii). (iii) follows from (i) and the Weinstein–Aronszajn identity,

$$\det \Sigma = \det(I_d - KH) \det Q = \det(I_m - HK) \det Q = \det(S - HQH^\top) \det S^{-1} \det Q,$$

while (iv) can be shown as follows:

$$\Delta_K S = K_t(S - S_t) + K_t S_t - QH^\top = -K_t H \Delta_Q H^\top + \Delta_Q H^\top = (I_d - K_t H) \Delta_Q H^\top.$$

Finally, using (i) as well as (ii), we obtain (v):

$$\begin{aligned} \Sigma_t &= (I - K_t H)Q(I - K_t H)^\top + K_t R K_t^\top \\ &= (I - KH - \Delta_K H)Q(I - KH - \Delta_K H)^\top + (K + \Delta_K)R(K + \Delta_K)^\top \\ &= \Sigma - \Delta_K H \Sigma - \Sigma H^\top \Delta_K^\top + \Delta_K H Q H^\top \Delta_K^\top + \Delta_K R K^\top + K R \Delta_K^\top + \Delta_K R \Delta_K^\top \\ &= \Sigma + \Delta_K (HQH^\top + R) \Delta_K^\top + \Delta_K (R K^\top - H \Sigma) + (K R - \Sigma H^\top) \Delta_K^\top \\ &= \Sigma + \Delta_K S \Delta_K^\top. \end{aligned}$$

⁶Note that the definition of Σ_t involves Q rather than Q_t . This is deliberate and not a typographical error.

Since $S \in \mathbf{S}_{++}^m$ and $\text{ran}(AA^\top) = \text{ran}(A)$ for every matrix A , $\text{ran} \Delta_\Sigma = \text{ran}(\Delta_K S^{1/2}) = \text{ran} \Delta_K$, while $\Delta_\Sigma \in \mathbf{S}_+^d$ and $\Sigma_t \in \mathbf{S}_{++}^d$ follow from $\Sigma_t \in \mathbf{S}_{++}^d$ and the above representation by considering the Loewner order. \blacksquare

Lemma C.2 (filtering component formula, cf. [Alspach and Sorenson 1972](#), Section III). *Under the assumptions of [Theorem 6.3](#) and using the notation therein, $\Sigma \in \mathbf{S}_{++}^d$ and*

$$p_t^{(i)} = \left(\frac{\det R}{\det S} \right)^{1/2} \exp \left(-\frac{1}{2} |y_t - Hf(x_{t-1}^{(i)})|_S^2 \right) \cdot \mathcal{N}(\hat{m}_t^{(i)}, \Sigma).$$

In other words, [Theorem 6.3\(a\)](#) holds.

Proof. $\Sigma \in \mathbf{S}_{++}^d$ was proven in [Theorem C.1\(iii\)](#). Denote $z = f(x_{t-1}^{(i)})$. By the Woodbury matrix identity as well as [Theorem C.1\(i\)](#) and (ii),

$$\begin{aligned} (H^\top R^{-1} H + Q^{-1})^{-1} &= Q - QH^\top(HQH^\top + R)^{-1}HQ = Q - KHQ &= \Sigma, \\ H^\top R^{-1} y_t + Q^{-1} z &= \Sigma^{-1}(Ky_t + (I_d - KH)z) &= \Sigma^{-1} \hat{m}_t^{(i)}, \\ R^{-1} - R^{-1} H \Sigma H^\top R^{-1} &= R^{-1} - R^{-1} H K &= R^{-1}(S - HQH^\top)S^{-1} = S^{-1}, \\ R^{-1} H \Sigma Q^{-1} &= R^{-1}(KR)^\top Q^{-1} &= S^{-1} HQQ^{-1} &= S^{-1} H, \\ Q^{-1} - Q^{-1} \Sigma Q^{-1} &= Q^{-1} - Q^{-1}(I - KH) &= Q^{-1} KH &= H^\top S^{-1} H. \end{aligned}$$

Using these identities and completing squares yields

$$\begin{aligned} I_t^{(i)}(x) &:= |Hx - y_t|_R^2 + |x - z|_Q^2 \\ &= x^\top (H^\top R^{-1} H + Q^{-1}) x - 2x^\top (H^\top R^{-1} y_t + Q^{-1} z) + |y_t|_R^2 + |z|_Q^2 \\ &= x^\top \Sigma^{-1} x - 2x^\top \Sigma^{-1} \hat{m}_t^{(i)} + |\hat{m}_t^{(i)}|_\Sigma^2 - |\hat{m}_t^{(i)}|_\Sigma^2 + |y_t|_R^2 + |z|_Q^2 \\ &= |x - \hat{m}_t^{(i)}|_\Sigma^2 + y_t^\top (R^{-1} - R^{-1} H \Sigma H^\top R^{-1}) y_t + z^\top (Q^{-1} - Q^{-1} \Sigma Q^{-1}) z - 2y_t^\top R^{-1} H \Sigma Q^{-1} z \\ &= |x - \hat{m}_t^{(i)}|_\Sigma^2 + y_t^\top S^{-1} y_t + z^\top H^\top S^{-1} H z - 2y_t^\top S^{-1} H z \\ &= |x - \hat{m}_t^{(i)}|_\Sigma^2 + |y_t - H z|_S^2. \end{aligned}$$

It follows from the definitions in (6.1) and (6.3) as well as [Theorem C.1\(iii\)](#) that

$$\begin{aligned} p_t^{(i)}(x) &= (2\pi)^{-d/2} \det Q^{-1/2} \exp \left(-\frac{1}{2} I_t^{(i)}(x) \right) \\ &= \det Q^{-1/2} \det \Sigma^{1/2} \exp \left(-\frac{1}{2} |y_t - H z|_S^2 \right) \cdot \mathcal{N}(\hat{m}_t^{(i)}, \Sigma) \\ &= \left(\frac{\det R}{\det S} \right)^{1/2} \exp \left(-\frac{1}{2} |y_t - H z|_S^2 \right) \cdot \mathcal{N}(\hat{m}_t^{(i)}, \Sigma). \end{aligned}$$

\blacksquare

Lemma C.3 (bound for target-proposal ratio). *Under the assumptions of [Theorem 6.3](#) and using the notation therein, there exists $u_t^{(i)} \in \mathbb{R}^d$ such that, for each $x \in \mathbb{R}^d$,*

$$\frac{p_t^{(i)}}{q_{p,t}^{(i)}}(x) \leq \left(\frac{\det \Sigma_{p,t}}{\det Q} \right)^{1/2} \exp \left(-\frac{1}{2} (x - u_t^{(i)})^\top (\Sigma^{-1} - \Sigma_{p,t}^{-1})(x - u_t^{(i)}) \right), \quad (\text{C.1})$$

with equality if $\text{Cov}^{\text{emp}}[(f(x_{t-1}^{(i)})_{i=1}^N)]$ is positive definite and H has full row rank. In other words, [Theorem 6.3\(b\)](#) holds.

Proof. Recall the definition of $q_{\mathbf{p},t}^{(i)} = \mathcal{N}(m_{\mathbf{p},t}^{(i)}, \Sigma_{\mathbf{p},t})$, cf. (5.8). To simplify notation, we drop the indices i and \mathbf{p} throughout the proof and denote $z = f(x_{t-1}^{(i)})$ and $w = y_t - Hz$. Since $A^\top (AA^\top)^\dagger A = A^\dagger A = \text{Proj}_{\text{ran } A^\top}$ for every matrix A , in particular for $A = \Delta_K S^{1/2}$, Theorem C.1(v) implies that

$$S^{-1} - \Delta_K^\top \Delta_\Sigma^\dagger \Delta_K = S^{-1/2} (I_m - A^\top (AA^\top)^\dagger A) S^{-1/2} = S^{-1/2} (I_m - \text{Proj}_{\text{ran}(S^{1/2} \Delta_K^\top)}) S^{-1/2} \in \mathbf{S}_+^m$$

is positive semidefinite. Since $m_t - \hat{m}_t = \Delta_K w$ and $\text{ran } \Delta_K = \text{ran } \Delta_\Sigma$ by Theorem C.1(v), it follows from Theorem C.5 that there exists $u \in \mathbb{R}^d$ such that

$$\begin{aligned} J_t(x) &:= |x - \hat{m}_t|_\Sigma^2 - |x - m_t|_{\Sigma_t}^2 + |w|_S^2 \\ &= (x - u)^\top (\Sigma^{-1} - \Sigma_t^{-1})(x - u) - (m_t - \hat{m}_t)^\top \Delta_\Sigma^\dagger (m_t - \hat{m}_t) + |w|_S^2 \\ &= (x - u)^\top (\Sigma^{-1} - \Sigma_t^{-1})(x - u) + w^\top (S^{-1} - \Delta_K^\top \Delta_\Sigma^\dagger \Delta_K) w \\ &\geq (x - u)^\top (\Sigma^{-1} - \Sigma_t^{-1})(x - u), \end{aligned}$$

with equality if and only if $w \in S^{1/2} \text{ran}(S^{1/2} \Delta_K^\top) = \text{ran}(H \Delta_Q (I_d - K_t H))$, where we used Theorem C.1(iv). $(I_d - K_t H)$ is invertible by the Weinstein–Aronszajn identity,

$$\det(I_d - K_t H) = \det(I_m - HK) = \det(S_t - HQ_t H^\top) \det S_t^{-1} = \det R \det S_t^{-1} > 0,$$

and therefore the above equality follows from the stated conditions: it holds whenever H has full row rank and $\text{Cov}^{\text{emp}}[(f(x_{t-1}^{(i)}))_{i=1}^N]$ is positive definite.

Setting $u_t^{(i)} := u$, the claim then follows from Theorem 6.3(a) and Theorem C.1(iii):

$$\frac{p_t^{(i)}}{Z^{\text{mix}} q_{\mathbf{p},t}^{(i)}}(x) = \left(\frac{\det R \det \Sigma_t}{\det S \det \Sigma} \right)^{1/2} \exp \left(-\frac{1}{2} J_t(x) \right) = \left(\frac{\det \Sigma_t}{\det Q} \right)^{1/2} \exp \left(-\frac{1}{2} J_t(x) \right).$$

■

Lemma C.4 (bound for IS weights). *Let the assumptions of Theorem 6.3 hold and consider the notation therein. For each $x \in \mathbb{R}^d$ and $i = 1, \dots, N$,*

$$\frac{p_t^{(i)}}{Z^{\text{mix}} q_{\mathbf{p},t}^{(i)}}(x) \leq \left(\frac{\det \hat{C}_t^{x,\mathbf{p}}}{\det Q} \right)^{1/2} \left(\frac{1}{N} \sum_{j=1}^N \exp \left(-\frac{1}{2} |y_t - Hf(x_{t-1}^{(j)})|_S^2 \right) \right)^{-1}. \quad (\text{C.2})$$

Further, for the sampling schemes $\text{II}_{\mathbf{p}}$ and $\text{MM}_{\mathbf{p}}^{\text{str}}$ defined in Algorithm 2, we have $\sigma_t^2 < \infty$ whenever f is bounded. In other words, Theorem 6.3(c) holds.

Proof. Since $Q_t \succcurlyeq Q$, $S_t \succcurlyeq S$ and

$$\tilde{\Sigma}_t := (I - K_t H) Q_t (I - K_t H)^\top + K_t R K_t^\top = \Sigma_t + (I - K_t H) \Delta_Q (I - K_t H)^\top \succcurlyeq \Sigma_t,$$

where \succcurlyeq denotes the Loewner order, a proof strategy identical to Theorem C.1(ii) yields

$$\det \Sigma_t \det S \leq \det \tilde{\Sigma}_t \det \tilde{S} = \det Q_t \det R. \quad (\text{C.3})$$

By Theorem C.1(v), $\Delta_\Sigma \in \mathbf{S}_+^d$, which implies that $\Sigma^{-1} - \Sigma_t^{-1} = \Sigma_t^{-1} \Delta_\Sigma \Sigma^{-1} \in \mathbf{S}_+^d$ holds, and (6.9),

$$p_t^{(i)} \leq \left(\frac{\det \Sigma_t}{\det Q} \right)^{1/2} q_{\mathbf{p},t}^{(i)}.$$

Moreover, by (6.8),

$$Z_t^{\text{mix}} = \frac{1}{N} \sum_{i=1}^N \int p_t^{(i)} = \left(\frac{\det R}{\det S} \right)^{1/2} \frac{1}{N} \sum_{i=1}^N \exp \left(-\frac{1}{2} |y_t - Hf(x_{t-1}^{(i)})|_S^2 \right).$$

Combining these observations, the ratio is bounded as

$$\frac{p_t^{(i)}}{Z_t^{\text{mix}} q_{p,t}^{(i)}} \leq \left(\frac{\det \Sigma_t \det S}{\det Q \det R} \right)^{1/2} \left(\frac{1}{N} \sum_{j=1}^N \exp \left(-\frac{1}{2} |y_t - Hf(x_{t-1}^{(j)})|_S^2 \right) \right)^{-1}$$

and (C.3) proves (C.2). Further, if f is bounded, then

$$c'_t := \sup_{(x^{(i)})_{i=1}^N \in (\mathbb{R}^d)^N} \frac{\det \hat{C}_t^{x,p}}{\det Q} < \infty, \quad c''_t := \sup_{x \in \mathbb{R}^d} e^{|y_t - Hf(x)|_S^2} < \infty,$$

where we used that $\hat{C}_t^{x,p} = Q + \mathbb{C}\text{ov}^{\text{emp}}[(f(x^{(i)}))_{i=1}^N]$ by (5.12). Therefore, for the scheme II_p , using (B.4),

$$\sigma_t^2 = \mathbb{E} \left[\left(\frac{\check{p}_t^{(i)}}{Z_t^{\text{mix}} \check{q}_t^{(i)}} \right)^2 \right] - 1 \leq c'_t c''_t - 1 < \infty.$$

For the scheme MM_p^{str} , $\sigma_t < \infty$ follows by Theorem 6.2. ■

Lemma C.5. *Let $A, B \in \mathbf{S}_{++}^d$ be symmetric and positive definite matrices, $a, b, v \in \mathbb{R}^d$ such that $(B - A)v = b - a$, and let $u = b - Bv$. Then, for all $x \in \mathbb{R}^d$,*

$$|x - a|_A^2 - |x - b|_B^2 = (x - u)^\top (A^{-1} - B^{-1})(x - u) - (b - a)^\top (B - A)^\dagger (b - a),$$

where $(B - A)^\dagger$ denotes the Moore—Penrose pseudoinverse.

Proof. Set $M := A^{-1} - B^{-1}$ and observe that

$$A^{-1}(b - a) = A^{-1}(B - A)v = (A^{-1} - B^{-1})Bv = MBv.$$

It follows for every $x \in \mathbb{R}^d$:

$$\begin{aligned} |x - a|_A^2 - |x - b|_B^2 &= |x - b + b - a|_A^2 - |x - b|_B^2 \\ &= (x - b)^\top (A^{-1} - B^{-1})(x - b) + 2(x - b)^\top A^{-1}(b - a) + |b - a|_A^2 \\ &= (x - b)^\top M(x - b) + 2(x - b)^\top MBv + (b - a)^\top A^{-1}(b - a) \\ &= (x - b + Bv)^\top M(x - b + Bv) - v^\top BMBv + v^\top (B - A)MBv \\ &= (x - u)^\top M(x - u) - v^\top AMBv. \end{aligned}$$

This proves the claim since

$$v^\top AMBv = v^\top (B - A)v = v^\top (B - A)(B - A)^\dagger (B - A)v = (b - a)^\top (B - A)^\dagger (b - a). ■$$

Acknowledgments

The authors acknowledge funding by the Deutsche Forschungsgemeinschaft (DFG, German Research Foundation) — CRC/TRR 388 “Rough Analysis, Stochastic Dynamics and Related Fields” — Project ID 516748464. The authors thank Jana de Wiljes and Tim Sullivan for helpful discussions and suggestions.

References

D. Alspach and H. Sorenson. Nonlinear Bayesian estimation using Gaussian sum approximations. *IEEE Transactions on Automatic Control*, 17(4):439–448, 1972. [doi:10.1109/TAC.1972.1100034](https://doi.org/10.1109/TAC.1972.1100034).

J. L. Anderson and S. L. Anderson. A Monte Carlo implementation of the nonlinear filtering problem to produce ensemble assimilations and forecasts. *Monthly Weather Review*, 127(12): 2741 – 2758, 1999. [doi:10.1175/1520-0493\(1999\)127<2741:AMCIOT>2.0.CO;2](https://doi.org/10.1175/1520-0493(1999)127<2741:AMCIOT>2.0.CO;2).

Y. Chen, W. Zhang, and M. Zhu. A localized weighted ensemble Kalman filter for high-dimensional systems. *Quarterly Journal of the Royal Meteorological Society*, 146(726):438–453, 2020. [doi:10.1002/qj.3685](https://doi.org/10.1002/qj.3685).

N. Chopin and O. Papaspiliopoulos. *An Introduction to Sequential Monte Carlo*. Springer, Cham, 2020. [doi:10.1007/978-3-030-47845-2](https://doi.org/10.1007/978-3-030-47845-2).

P. Del Moral and E. Horton. A theoretical analysis of one-dimensional discrete generation ensemble Kalman particle filters. *Ann. Appl. Probab.*, 33(2):1127–1172, 2023. [doi:10.1214/22-aap1843](https://doi.org/10.1214/22-aap1843).

A. Doucet and A. M. Johansen. A tutorial on particle filtering and smoothing: fifteen years later. In *The Oxford handbook of nonlinear filtering*, pages 656–704. Oxford Univ. Press, Oxford, 2011.

A. Doucet, N. de Freitas, and N. Gordon, editors. *Sequential Monte Carlo Methods in Practice*. Springer, New York, NY, 2001. [doi:10.1007/978-1-4757-3437-9](https://doi.org/10.1007/978-1-4757-3437-9).

G. Evensen. Sequential data assimilation with a nonlinear quasi-geostrophic model using Monte Carlo methods to forecast error statistics. *Journal of Geophysical Research: Oceans*, 99(C5): 10143–10162, 1994. [doi:10.1029/94JC00572](https://doi.org/10.1029/94JC00572).

G. Evensen. The ensemble Kalman filter: theoretical formulation and practical implementation. *Ocean Dynamics*, 53(4):343–367, 2003. [doi:10.1007/s10236-003-0036-9](https://doi.org/10.1007/s10236-003-0036-9).

G. Evensen, F. C. Vossepoel, and P. J. van Leeuwen. *Data assimilation fundamentals—a unified formulation of the state and parameter estimation problem*. Springer Textbooks in Earth Sciences, Geography and Environment. Springer, Cham, 2022. [doi:10.1007/978-3-030-96709-3](https://doi.org/10.1007/978-3-030-96709-3).

M. Frei and H. R. Künsch. Mixture ensemble Kalman filters. *Comput. Statist. Data Anal.*, 58: 127–138, 2013a. [doi:10.1016/j.csda.2011.04.013](https://doi.org/10.1016/j.csda.2011.04.013).

M. Frei and H. R. Künsch. Bridging the ensemble Kalman and particle filters. *Biometrika*, 100 (4):781–800, 2013b. URL <https://doi.org/10.1093/biomet/ast020>.

N. Gordon, D. Salmond, and A. Smith. Novel approach to nonlinear/non-Gaussian Bayesian state estimation. *IEE Proceedings F (Radar and Signal Processing)*, 140:107–113, 1993. [doi:10.1049/ip-f-2.1993.0015](https://doi.org/10.1049/ip-f-2.1993.0015).

A. Gretton, K. M. Borgwardt, M. J. Rasch, B. Schölkopf, and A. Smola. A kernel two-sample test. *J. Mach. Learn. Res.*, 13:723–773, 2012. URL <http://jmlr.org/papers/v13/gretton12a.html>.

I. Grooms and G. Robinson. A hybrid particle-ensemble Kalman filter for problems with medium nonlinearity. *PLOS ONE*, 16(3):1–20, 03 2021. [doi:10.1371/journal.pone.0248266](https://doi.org/10.1371/journal.pone.0248266).

T. M. Hamill, J. S. Whitaker, and C. Snyder. Distance-dependent filtering of background error covariance estimates in an ensemble Kalman filter. *Monthly Weather Review*, 129(11):2776 – 2790, 2001. [doi:10.1175/1520-0493\(2001\)129<2776:DDFOBE>2.0.CO;2](https://doi.org/10.1175/1520-0493(2001)129<2776:DDFOBE>2.0.CO;2).

I. Hoteit, X. Luo, and D.-T. Pham. Particle Kalman filtering: A nonlinear Bayesian framework for ensemble Kalman filters. *Monthly Weather Review*, 140(2):528 – 542, 2012. [doi:10.1175/2011MWR3640.1](https://doi.org/10.1175/2011MWR3640.1).

P. L. Houtekamer and H. L. Mitchell. A sequential ensemble Kalman filter for atmospheric data assimilation. *Monthly Weather Review*, 129(1):123 – 137, 2001. [doi:10.1175/1520-0493\(2001\)129<0123:ASEKFF>2.0.CO;2](https://doi.org/10.1175/1520-0493(2001)129<0123:ASEKFF>2.0.CO;2).

I. Klebanov and T. J. Sullivan. Transporting higher-order quadrature rules: Quasi-Monte Carlo points and sparse grids for mixture distributions, 2023. [arXiv:2308.10081](https://arxiv.org/abs/2308.10081).

K. Law, A. Stuart, and K. Zygalakis. *Data assimilation*, volume 62 of *Texts in Applied Mathematics*. Springer, Cham, 2015. ISBN 978-3-319-20324-9; 978-3-319-20325-6. [doi:10.1007/978-3-319-20325-6](https://doi.org/10.1007/978-3-319-20325-6). A mathematical introduction.

E. N. Lorenz. Deterministic nonperiodic flow. *J. Atmospheric Sci.*, 20(2):130–141, 1963. [doi:10.1175/1520-0469\(1963\)020<0130:DNF>2.0.CO;2](https://doi.org/10.1175/1520-0469(1963)020<0130:DNF>2.0.CO;2).

E. N. Lorenz. Predictability: A problem partly solved. In *Proc. Seminar on predictability*, volume 1, pages 1–18. Reading, 1996.

J. Matoušek. On the L_2 -discrepancy for anchored boxes. *J. Complexity*, 14(4):527–556, 1998. [doi:10.1006/jcom.1998.0489](https://doi.org/10.1006/jcom.1998.0489).

M. Morzfeld, D. Hodyss, and C. Snyder. What the collapse of the ensemble Kalman filter tells us about particle filters. *Tellus A: Dynamic Meteorology and Oceanography*, 69(1):1283809, 2017. [doi:10.1080/16000870.2017.1283809](https://doi.org/10.1080/16000870.2017.1283809).

J. D. Murray. *Mathematical biology. I*, volume 17 of *Interdisciplinary Applied Mathematics*. Springer-Verlag, New York, third edition, 2002. [doi:10.1007/b98868](https://doi.org/10.1007/b98868). An introduction.

A. Owen and Y. Zhou. Safe and effective importance sampling. *J. Amer. Statist. Assoc.*, 95(449):135–143, 2000. [doi:10.2307/2669533](https://doi.org/10.2307/2669533).

A. B. Owen. Randomly permuted (t, m, s) -nets and (t, s) -sequences. In *Monte Carlo and quasi-Monte Carlo methods in scientific computing (Las Vegas, NV, 1994)*, volume 106 of *Lect. Notes Stat.*, pages 299–317. Springer, New York, 1995. [doi:10.1007/978-1-4612-2552-2_19](https://doi.org/10.1007/978-1-4612-2552-2_19).

A. B. Owen. Scrambling Sobol' and Niederreiter-Xing points. *J. Complexity*, 14(4):466–489, 1998. [doi:10.1006/jcom.1998.0487](https://doi.org/10.1006/jcom.1998.0487).

A. B. Owen. *Monte Carlo Theory, Methods and Examples*. 2013. Available online: <https://artowen.su.domains/mc/>.

N. Papadakis, E. Mémin, A. Cuzol, and N. Gengembre. Data assimilation with the weighted ensemble Kalman filter. *Tellus A: Dynamic Meteorology and Oceanography*, 62(5):673–697, 2010. [doi:10.1111/j.1600-0870.2010.00461.x](https://doi.org/10.1111/j.1600-0870.2010.00461.x).

D. Pasetto, M. Camporese, and M. Putti. Ensemble Kalman filter versus particle filter for a physically-based coupled surface–subsurface model. *Advances in Water Resources*, 47:1–13, 2012. [doi:10.1016/j.advwatres.2012.06.009](https://doi.org/10.1016/j.advwatres.2012.06.009).

S. Reich. A nonparametric ensemble transform method for Bayesian inference. *SIAM J. Sci. Comput.*, 35(4):A2013–A2024, 2013. [doi:10.1137/130907367](https://doi.org/10.1137/130907367).

C. Robert and H. R. Künsch. Localizing the ensemble Kalman particle filter. *Tellus A: Dynamic Meteorology and Oceanography*, 69(1):1282016, 2017. [doi:10.1080/16000870.2017.1282016](https://doi.org/10.1080/16000870.2017.1282016).

R. Y. Rubinstein and D. P. Kroese. *Simulation and the Monte Carlo Method*. Wiley Series in Probability and Statistics. John Wiley & Sons, Inc., Hoboken, NJ, third edition, 2016. [doi:10.1002/9781118631980](https://doi.org/10.1002/9781118631980).

D. Sanz-Alonso, A. Stuart, and A. Taeb. *Inverse problems and data assimilation*, volume 107 of *London Mathematical Society Student Texts*. Cambridge University Press, Cambridge, 2023. [doi:10.1017/9781009414319](https://doi.org/10.1017/9781009414319).

L. Slivinski, E. Spiller, A. Apte, and B. Sandstede. A hybrid particle–ensemble Kalman filter for Lagrangian data assimilation. *Monthly Weather Review*, 143(1):195 – 211, 2015. [doi:10.1175/MWR-D-14-00051.1](https://doi.org/10.1175/MWR-D-14-00051.1).

A. S. Stordal, H. A. Karlsen, G. Nævdal, H. J. Skaug, and B. Vallès. Bridging the ensemble Kalman filter and particle filters: The adaptive Gaussian mixture filter. *Computational Geosciences*, 15(2):293–305, 2011. [doi:10.1007/s10596-010-9207-1](https://doi.org/10.1007/s10596-010-9207-1).

A. Taghvaei and P. G. Mehta. An optimal transport formulation of the ensemble Kalman filter. *IEEE Transactions on Automatic Control*, 66(7):3052–3067, 2021. [doi:10.1109/TAC.2020.3015410](https://doi.org/10.1109/TAC.2020.3015410).

P. J. van Leeuwen, H. R. Künsch, L. Nerger, R. Potthast, and S. Reich. Particle filters for high-dimensional geoscience applications: A review. *Quarterly Journal of the Royal Meteorological Society*, 145(723):2335–2365, 2019. [doi:10.1002/qj.3551](https://doi.org/10.1002/qj.3551).

E. Veach and L. J. Guibas. Optimally combining sampling techniques for Monte Carlo rendering. In *Proceedings of the 22nd Annual Conference on Computer Graphics and Interactive Techniques*, SIGGRAPH '95, page 419–428, New York, NY, USA, 1995. Association for Computing Machinery. [doi:10.1145/218380.218498](https://doi.org/10.1145/218380.218498).

J. S. Whitaker and T. M. Hamill. Evaluating methods to account for system errors in ensemble data assimilation. *Monthly Weather Review*, 140(9):3078 – 3089, 2012. [doi:10.1175/MWR-D-11-00276.1](https://doi.org/10.1175/MWR-D-11-00276.1).